

**UNIVERSITÀ DEGLI STUDI DI PADOVA**

**Dipartimento di Fisica e Astronomia “Galileo Galilei”**

**Corso di Laurea in Fisica**

**Tesi di Laurea**

**Elementary excitations and quantized vortices in  
bosonic superfluids**

**Relatore**

**Prof. Luca Salasnich**

**Laureando**

**Alessandro Lenoci**

**Anno Accademico 2017/2018**



# Contents

<b>1</b>	<b>Bosonic superfluids</b>	<b>4</b>
1.1	BEC, ultra-cold alkali gases and superfluid $^4\text{He}$ . . . . .	4
1.2	Hartree equation . . . . .	6
1.3	Scattering theory and finite range approximation . . . . .	9
<b>2</b>	<b>Elementary excitations</b>	<b>13</b>
2.1	Superfluid behavior and Landau's criterion . . . . .	13
2.2	Quasiparticle dispersion relation . . . . .	15
2.3	Excitation spectrum for a weakly-interacting Bose gas . . . . .	16
2.4	Excitation spectrum for superfluid $^4\text{He}$ . . . . .	18
<b>3</b>	<b>Quantized vortices</b>	<b>21</b>
3.1	Phase defects and vortices . . . . .	21
3.2	Vortices in dilute weakly interacting Bose gases . . . . .	22
3.3	Vortices in superfluid $^4\text{He}$ . . . . .	25

# Introduction

Since the last century much theoretical work in the context of statistic quantum mechanics has been done to explain phenomena such as Bose-Einstein condensation (BEC), superconductivity and superfluidity. These are commonly called macroscopic quantum phenomena as their properties are consequences of quantum mechanics effects that occur below a critical temperature and affect the bulk properties of matter on a large scale. While BEC has been only a theoretical prediction for more than seventy years, the existence of superfluidity was experimentally observed with the  $\lambda$ -transition of  $^4\text{He}$  and confirmed at the very beginning of low temperature's physics studies by Kapitza in 1938 [1], who introduced the term 'superfluidity' characterizing the ability to flow through narrow channels in absence of viscosity. Soon after this discovery, London [2] established a relation between the  $\lambda$ -transition and BEC of  $^4\text{He}$  bosons suggesting the existence of a classical field  $\Psi$ , the order parameter and the wave function associated with the macroscopic component of the field operator. This idea was developed with the two fluid model by Landau [3] and Tisza [4] and led to a successful theory of motion for superfluid helium which also considered quasiparticle excitations. Subsequently more phenomena related to superfluidity were investigated, as quantized vortices, whose existence was predicted by Onsager [5] and Feynman [6] in the 1950s. Another important step towards the comprehension of macroscopic quantum phenomena was taken with BCS theory (1957) by Bardeen, Cooper and Schrieffer, which extended BEC to fermionic systems with the condensations of Cooper pairs behaving like a boson state.

In the experimental field many efforts were aimed at obtaining BEC. In 1980s progresses in cooling and trapping techniques through magnetic traps and optical lattices allowed to reach the necessary values of temperature and density in order to observe BEC. The purpose was finally achieved in 1995 with atomic vapours of  $^{87}\text{Rb}$  [7] and  $^{23}\text{Na}$  [8] and earning Cornell, Wieman and Ketterle the Nobel prize (2001). The discovery opened a new chapter in condensed matter physics and since then many groups have observed BEC with trapped dilute and ultra-cold alkali atoms: these systems also show superfluid properties with some differences compared to the case of  $^4\text{He}$ , mainly due to the interaction potential between atoms. Techniques developed in the recent years, such as Feshbach resonances [9], provide the possibility to vary the parameters characterizing the atomic interaction and to observe via experiments many quantum effects in peculiar regimes and many other superfluid systems (Fermi gas, polariton condensates, multi-component BECs), hence the importance of theoretical work in this scope.

The purpose of this work is to study two systems of bosonic superfluids at zero temperature, ultra-cold Bose gases and superfluid helium, within a simple classical field formalism, to underline differences and similarities between them. We will start in general from the Hartree equation of a bosonic system and, with different hypothesis on the interaction potential between bosons, we will obtain the equations describing the two systems, mainly focusing on elementary quasiparticle excitations and quantized vortices. As we shall see, modeling  $^4\text{He}$  is much more difficult than modeling a weakly interacting Bose gas since, in that case, the mean-field approach of the usually employed GP theory [10] [11] is not appropriate to describe the main properties of superfluid helium. So our efforts will be

mainly directed to modeling  $^4\text{He}$  with the help of theories developed in the last two decades. Furthermore throughout this work the results will be compared with experimental data and aftermaths of theories in literature, mainly the GP theory and its modifications for weakly-interacting Bose gases, the density functional theory by Dalfovo [12], [13], and non-local non-linear model proposed by Berloff for helium [14].

The author would like to thank Luca Salasnich for many useful discussions and informations, Annachiara Picco for support and many advices and Brendan B. Godfrey for the precious computational help in solving ODEs involving a separatrix problem.

*“That is one of the challenges of  
the shooting method: some of  
the shots can be way off target.”*

– Brendan B. Godfrey

# 1

## Bosonic superfluids

In this chapter we will point out the concepts and develop the tools we will use to investigate the features of bosonic superfluids. In the first section we will study the main properties of Bose-Einstein condensates, superfluid  $^4\text{He}$  and ultra-cold atomic gases with the help of some of the theories developed in literature. In the second section we will obtain the Hartree equation for bosons at zero temperature and, with different choices of pseudopotentials, the Gross-Pitaevskii equation (GPE). In the third section we will study with the help of scattering theory the parameters characterizing the interaction potential for Bose gases, such as the scattering length and the effective range and we will obtain a modified Gross-Pitaevskii equation (MGPE) suitable to describe ultra-cold dilute Bose gases.

### 1.1 BEC, ultra-cold alkali gases and superfluid $^4\text{He}$

Unlike the ideal classical gas, the Bose-Einstein non-interacting gas, if cooled below a critical temperature  $T_c$ , has a thermodynamic phase transition due only to the particle statistics. BEC is usually interpreted as a first-order phase transition and is a state of matter in which a large fraction  $n_0$  of bosons collapse into its lowest quantum state: the separation of the two phases occurs in momentum space [2], where the condensed bosons occupy a single quantum state with zero momentum  $\mathbf{p} = \hbar\mathbf{q} = 0$  and the normal particles have finite momentum.

After the discovery of superfluidity of liquid helium below the temperature  $T_\lambda \simeq 2.17$  K, since  $^4\text{He}$  atoms are bosons, and from calculations  $T_c$  is close to  $T_\lambda$ , suggesting a relationship between BEC and superfluidity was quite natural. Nevertheless BEC was predicted for an ideal Bose gas, in which interactions between the atoms can be neglected, while liquid helium is, as we shall see, a strongly-interacting system, due to the interatomic potential and the high density  $n = 0.0218 \text{ \AA}^{-3}$ . That is why BEC was not achieved via experiments with helium but with very dilute ultra-cold gases of alkali atoms instead.

This kind of atoms is particularly suitable for observing BEC because they can be cooled in magnetic traps in order to obtain very low densities of order  $10^{-13} - 10^{-9} \text{ \AA}^{-3}$  and for these densities we expect  $T_c$  of the order of  $10^{-6} - 10^{-9}$  K. The magnetic trap method employs the energy difference between different states of total spin (composition of nuclear and valence electron spins), due to hyperfine interaction, to keep the 'low energy atoms' bounded to the trap, letting the 'high energy atoms' escape instead, so the system will cool in average by evaporation. However an alkali atom gas is not an ideal Bose gas because the interactions between trapped atoms cannot be neglected: the atoms show a strong repulsion at short distance and a Van der Waals attractive force at long distances. Nevertheless, the rate of three-body collisions (that could lead to binding) is very slow due to the extremely low densities of these gases, and so the interaction potential is well approximated by the

pseudopotential

$$V(\mathbf{r} - \mathbf{r}') = g_0 \delta(\mathbf{r} - \mathbf{r}'), \quad (1.1)$$

where the parameter  $g_0$  defines the strength of the interaction. So a mean-field approach to the study of a dilute alkali gas is possible and, as we shall see, the GP theory works well in describing these systems' properties and phenomena, such as quantized vortices. The fact that a dilute alkali gas is a weakly interacting system and not a non-interacting one is crucial: the two-body interactions are not just necessary to reach the thermal equilibrium but they assure superfluidity in the condensate too. As we shall see in chapter 2, in absence of interactions, the critical Landau velocity of the superfluid is zero, hence it is impossible to have a flow with zero viscosity.

Unlike dilute alkali gases, liquid helium is a strongly interacting system due to its high density. It also has peculiar features such as the fact that it remains in the liquid state down to 0 K for pressures below about 2.5 MPa, as we can see from the phase diagram of  $^4\text{He}$  in Fig. (1.1): there are two different phases, the normal liquid He I and the superfluid liquid He II, and no triple point. Liquid helium is a clear example of a quantum fluid in which the effects of quantum mechanics are dominant: this is the result of the light mass of  $^4\text{He}$  atoms and the weak attractive Van der Waals interactions. Near the minimum of the attracting well the interaction potential of helium is well described by a 12-6 Lennard-Jones profile (for a more accurate potential see [15])

$$V(r) = 4\epsilon \left[ \left( \frac{\alpha}{r} \right)^{12} - \left( \frac{\alpha}{r} \right)^6 \right], \quad (1.2)$$

with  $\epsilon = 10.22$  K and  $\alpha = 2.556 \text{ \AA}$ : the little value of  $\epsilon$  makes helium liquid only at 4 K. To give an estimate of the role of quantum effects in the two phase we compute the thermal de Broglie wavelength at  $T \simeq 4$  K

$$\lambda_{\text{dB}} = \sqrt{\frac{2\pi\hbar^2}{mk_{\text{B}}T}} \simeq 4 \text{ \AA}.$$

Since it is greater than the interatomic distance  $d = n^{-1/3} \simeq 3.5 \text{ \AA}$ , quantum effects are really important in liquid helium. The fact that helium remains liquid down to 0 K is due to zero point motion characterizing quantum fluids [16], [6], so that the solid phase only occurs when high pressures are applied.

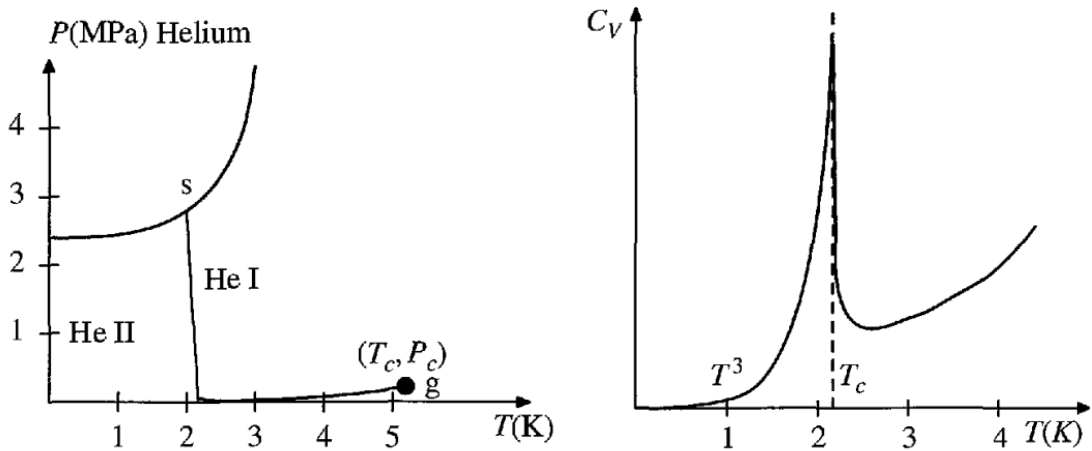


Figure 1.1: Left: phase diagram of  $^4\text{He}$  showing the two phases He I and He II. Right: specific heat  $C_V$  of  $^4\text{He}$  showing the  $\lambda$ -transition. Figures taken from Annett. [16]

Another important feature of liquid helium is the specific heat  $C_V$  singularity at the boundary between the two phases He I and He II around  $T_\lambda \simeq 2.17$  K, as shown in Fig. (1.1)

which is called  $\lambda$ -point because of its form. The singularity is well described by a power law:  $C_V \simeq |T - T_\lambda|^{-0.009}$ . Such power laws are very common in phase transitions and many systems share the same sets of critical exponents: this is due to the fact that, below a critical temperature, different systems show a sort of order which, in the case of He II and also for BECs, can be interpreted as the presence of a coherence direction  $\theta$ . This direction  $\theta(\mathbf{r})$  (that in general can be a function of coordinates) corresponds to the phase of a macroscopic wave function  $\psi(\mathbf{r}, t) = |\psi(\mathbf{r}, t)|e^{i\theta(\mathbf{r}, t)}$  that can be seen as the order parameter of the He II phase. Working at  $T = 0$  K, if  $\psi$  is normalized to the total number of particles  $N$

$$N = \int d^3\mathbf{r} |\psi(\mathbf{r})|^2, \quad (1.3)$$

where  $n$  is the total density, we can write the wave function of the superfluid phase in the useful form

$$\psi(\mathbf{r}, t) = \sqrt{n(\mathbf{r})} e^{i\theta(\mathbf{r}, t)}, \quad (1.4)$$

known as Madelung transform: we shall see that this expression contains informations on superfluid flow and quantized vortices. However we should clarify why we used the total density  $n$  in the Madelung transform. Experiments on the superfluidity of He II showed that this phase is well described by a two-fluid model [3], [4], so we can divide the total density in two components: the "superfluid" component and the "normal" one:

$$n = n_s + n_n. \quad (1.5)$$

At zero temperature it can be shown that  $n_s = n$  and  $n_n = 0$ , meaning that all the particles participate in superflow. We also must not confuse the superfluid density  $n_s$  with the condensate density  $n_0$ , which for helium at zero temperature is only a small fraction of the total,  $n_0 \simeq 0.1n$ . This distinguishes liquid helium from weakly interacting Bose gases such as ultra-cold alkali atoms, for which is proved that at zero temperature  $n_0 = n_s \simeq n$ : it is due to the strong interactions between  $^4\text{He}$  atoms again. Indeed, in general, at zero temperature the total number density  $n$  of a bosonic system can be written as

$$n = n_0 + n_1, \quad (1.6)$$

where  $n_1$  is the number density of the bosons out of the condensate. Now we want to use these concepts to obtain an equation that describes as many of the system's properties as possible.

## 1.2 Hartree equation

Let us consider a system composed by  $N$  bosons in the same spin state. The system is described by a symmetrical many-body wave function  $\Psi$  depending on spatial coordinates  $\mathbf{r}_i = (x_i, y_i, z_i)$  of the  $i$ -th particle and on time  $t$ :

$$\Psi = \Psi(\mathbf{r}_1, \mathbf{r}_2, \dots, \mathbf{r}_N, t).$$

The system's dynamics is described by the many-body Schrödinger equation (SE)

$$i\hbar \frac{\partial}{\partial t} \Psi = H \Psi,$$

with  $H$  the system's hamiltonian. Let us verify that the SE can be obtained extremizing the following functional called Dirac's action.

$$S_D[\Psi, \Psi^*] = \int_{t_1}^{t_2} dt \int d^3\mathbf{r}_1 \dots d^3\mathbf{r}_N \Psi^*(\mathbf{r}_1, \mathbf{r}_2, \dots, \mathbf{r}_N, t) \left[ i\hbar \frac{\partial}{\partial t} - H \right] \Psi(\mathbf{r}_1, \mathbf{r}_2, \dots, \mathbf{r}_N, t).$$



Imposing  $\forall \delta\Psi$  such that  $\delta\Psi(\mathbf{r}, t_1) = \delta\Psi(\mathbf{r}, t_2) = 0$ , we have

$$\delta S_D = \frac{d}{d\alpha} S_D[\Psi + \alpha\delta\Psi, \Psi^* + \alpha\delta\Psi^*] \Big|_{\alpha=0} = 0,$$

and we obtain

$$\delta S_D = \int_{t_1}^{t_2} dt \int d^3\mathbf{r}_1 \dots d^3\mathbf{r}_N \delta\Psi^* \left[ i\hbar \frac{\partial}{\partial t} - H \right] \Psi + \text{c.c.} = 0,$$

where c.c. is the conjugate complex. So  $\delta S_D = 0$  if and only if the SE is satisfied.

Now we want to obtain an equation describing the ground state and excitation properties (elementary excitations and quantized vortices) of a general superfluid system of  $N$  bosons. We will try to maintain the most possibly general point of view within our classical field formalism. Firstly let us consider a weakly interacting Bose gas. At zero temperature we can consider all the bosons in their lowest single-particle quantum state, so we have a wave function given by the Hartree approximation:

$$\Psi(\mathbf{r}_1, \mathbf{r}_2, \dots, \mathbf{r}_N, t) = \prod_{i=1}^N \psi(\mathbf{r}_i, t). \quad (1.7)$$

This ansatz is very useful because it allows to reduce the many-body problem to a single particle wave function's equation. Now we write the system's Hamiltonian:

$$H = \sum_{i=1}^N \left[ -\frac{\hbar^2}{2m} \nabla_i^2 + V_{\text{ext}}(\mathbf{r}_i) \right] + \frac{1}{2} \sum_{i \neq j}^N V(\mathbf{r}_i, \mathbf{r}_j), \quad (1.8)$$

where  $V_{\text{ext}}$  is an external trapping potential and  $V$  is a two-body interaction potential. Writing the Dirac action for the system described and substituting the Hartree approximation ansatz for the wave function Eq. (1.7), we find

$$S_D[\psi, \psi^*] = N \int_{t_1}^{t_2} dt \int d^3\mathbf{r} \psi^*(\mathbf{r}, t) \left[ i\hbar \frac{\partial}{\partial t} + \frac{\hbar^2}{2m} \nabla^2 - V_{\text{ext}}(\mathbf{r}) - \frac{N-1}{2} \int d^3\mathbf{r}' V(\mathbf{r}, \mathbf{r}') |\psi(\mathbf{r}', t)|^2 \right] \psi(\mathbf{r}, t). \quad (1.9)$$

Considering the thermodynamic limit  $N-1 \simeq N$  and choosing the normalization of the single particle wave function

$$N = \int d^3\mathbf{r} |\psi(\mathbf{r})|^2, \quad (1.10)$$

the action takes the form

$$S_D[\psi, \psi^*] = \int_{t_1}^{t_2} dt \int d^3\mathbf{r} \left\{ \psi^*(\mathbf{r}, t) \left[ i\hbar \frac{\partial}{\partial t} + \frac{\hbar^2}{2m} \nabla^2 - V_{\text{ext}}(\mathbf{r}) - \frac{1}{2} \int d^3\mathbf{r}' V(\mathbf{r}, \mathbf{r}') |\psi(\mathbf{r}', t)|^2 \right] \psi(\mathbf{r}, t) \right\}. \quad (1.11)$$

We can now proceed to find the equations associated to this action by extremizing it:

$$\delta S_D = \int_{t_1}^{t_2} dt \int d^3\mathbf{r} \delta\psi^* \left[ i\hbar \frac{\partial}{\partial t} + \frac{\hbar^2}{2m} \nabla^2 - V_{\text{ext}}(\mathbf{r}) - \int d^3\mathbf{r}' V(\mathbf{r}, \mathbf{r}') |\psi(\mathbf{r}', t)|^2 \right] \psi + \text{c.c.} = 0. \quad (1.12)$$

In conclusion we obtain

$$i\hbar \frac{\partial}{\partial t} \psi(\mathbf{r}, t) = \left[ -\frac{\hbar^2}{2m} \nabla^2 + V_{\text{ext}}(\mathbf{r}) + \int d^3\mathbf{r}' V(\mathbf{r}, \mathbf{r}') |\psi(\mathbf{r}', t)|^2 \right] \psi(\mathbf{r}, t), \quad (1.13)$$

called the Hartree equation for weakly interacting Bose gas with general interaction potential  $V(\mathbf{r}, \mathbf{r}')$ . As stated in the previous section, for a trapped ultra-cold and dilute Bose gas we can consider a mean-field interaction pair pseudopotential  $V(\mathbf{r}, \mathbf{r}') = g_0 \delta(|\mathbf{r} - \mathbf{r}'|)$ . Hence Eq. (1.23) reduces to the well-known Gross-Pitaevskii equation (GPE):

$$i\hbar \frac{\partial}{\partial t} \psi(\mathbf{r}, t) = \left[ -\frac{\hbar^2}{2m} \nabla^2 + V_{\text{ext}}(\mathbf{r}) + g_0 |\psi(\mathbf{r}, t)|^2 \right] \psi(\mathbf{r}, t). \quad (1.14)$$

In section 1.3 we shall slightly improve this model taking into account finite range interaction.

Inspired by many successes of this approach to the dilute alkali Bose gases we want to try to model superfluid helium with a similar single particle formalism. For a strongly interacting system, the condensate wave function, which we shall call  $\Phi_0$ , cannot be obtained by the Hartree approximation ansatz in Eq. (1.7) for the many body wave function  $\Psi$ . In general, the most rigorous approach to commuting the many-body problem in a single-particle one in BEC is the one reported by Leggett in his review [17]. Following the author, we write the one-particle density function

$$G(\mathbf{r}, \mathbf{r}', t) = \int d^3\mathbf{r}_1 \dots d^3\mathbf{r}_N \Psi^*(\mathbf{r}, \mathbf{r}_2, \dots, \mathbf{r}_N, t) \Psi(\mathbf{r}', \mathbf{r}_2, \dots, \mathbf{r}_N, t). \quad (1.15)$$

Since from its definition  $G(\mathbf{r}, \mathbf{r}', t)$ , when regarded as a matrix function of indices  $\mathbf{r}$  and  $\mathbf{r}'$ , is Hermitian, it is always possible to find a complete orthonormal basis of single-particle eigenfunctions  $\Phi_j$  such that

$$G(\mathbf{r}, \mathbf{r}', t) = \sum_j N_j \Phi_j^*(\mathbf{r}, t) \Phi_j(\mathbf{r}', t) \quad (1.16)$$

and that the eigenvalue equation is satisfied:

$$\int d^3\mathbf{r}' G(\mathbf{r}, \mathbf{r}', t) \Phi_j(\mathbf{r}', t) = N_j \Phi_j(\mathbf{r}, t). \quad (1.17)$$

We can say that the system shows BEC if one or more of the eigenvalues  $N_j$  is of the order of the total number of particles  $N$ ; considering the largest eigenvalue  $N_0$  and supposing we are able to solve the Eq. (1.17), we can find the condensate single particle wave function  $\Phi_0$ . To be rigorous, notice that the phase of  $\Phi_0$  is the one appearing in the Madelung transform of the macroscopic wave function Eq. (1.4). Unlike the weakly interacting case, in which  $\Phi_0(\mathbf{r}, t)$  is substantially equal to the Hartree approximation single-particle wave functions  $\psi(\mathbf{r}, t)$ , in the case of He II there is not such equality since at zero temperature the number of condensate bosons is only a small fraction of the total number of particles. So, in order to model superfluid helium within the single particle approach, we assume to be able to solve Eq. (1.17) for  $j = 0$  to find  $\Phi_0$  and then we define the single-particle wave function as

$$\psi(\mathbf{r}, t) = \sqrt{N} \Phi_0(\mathbf{r}, t), \quad (1.18)$$

where  $N$  is the total number of particles and where  $\Phi_0(\mathbf{r}, t)$  is normalized to 1. In this way we expect this wave function to embody all the superfluid properties of He II since, as seen in the previous section, at zero temperature  $n = n_s$ . In order to obtain a more general Hartree equation for liquid helium, we assume we can write the action as the sum of two contributions: the condensate-like action  $S_0$ , which depends on the just defined wave function  $\psi(\mathbf{r}, t)$ , and the out-of-condensate-like action  $S_1$ , which depends only on the total number density  $n$  of the system:

$$S[\psi, \psi^*; n] = S_1(n) + S_0[\psi, \psi^*], \quad (1.19)$$

with

$$S_1(n) = - \int_{t_1}^{t_2} dt \int d^3\mathbf{r} \varepsilon_1(n), \quad (1.20)$$

where  $\varepsilon_1(n)$  is the energy density contribution due to the out-of-condensate bosonic particles. We can write the action  $S_0$  as

$$S_0[\psi, \psi^*] = S_D[\psi, \psi^*] - \int_{t_1}^{t_2} dt \int d^3\mathbf{r} \varepsilon_{\text{corr}}(|\psi|^2), \quad (1.21)$$

in which we added a correlation term  $\varepsilon_{\text{corr}}(|\psi|^2)$  that will be useful in modeling  $^4\text{He}$ . By extremizing Eq. (1.21), as previously done in the weakly interacting case, but taking into account the additional term

$$\delta S_0 = \int_{t_1}^{t_2} dt \int d^3\mathbf{r} \delta\psi^* \left[ i\hbar \frac{\partial}{\partial t} + \frac{\hbar^2}{2m} \nabla^2 - V_{\text{ext}}(\mathbf{r}) - \int d^3\mathbf{r}' V(\mathbf{r}, \mathbf{r}') |\psi(\mathbf{r}', t)|^2 - \mu_{\text{corr}}(|\psi|^2) \right] \psi + \text{c.c.} = 0, \quad (1.22)$$

we find

$$i\hbar \frac{\partial}{\partial t} \psi(\mathbf{r}, t) = \left[ -\frac{\hbar^2}{2m} \nabla^2 + V_{\text{ext}}(\mathbf{r}) + \int d^3\mathbf{r}' V(\mathbf{r}, \mathbf{r}') |\psi(\mathbf{r}', t)|^2 + \mu_{\text{corr}}(|\psi|^2) \right] \psi(\mathbf{r}, t), \quad (1.23)$$

which is the general Hartree equation that we will employ in modeling  $^4\text{He}$ . The energy of the system can be obtained from Eq. (1.19):

$$E[\psi, \psi^*; n] = \int d^3\mathbf{r} \left[ \frac{\hbar^2}{2m} |\nabla\psi|^2 + V_{\text{ext}}(\mathbf{r}) |\psi|^2 + \frac{1}{2} \int d^3\mathbf{r}' |\psi(\mathbf{r}, t)|^2 V(\mathbf{r}, \mathbf{r}') |\psi(\mathbf{r}', t)|^2 + \varepsilon_{\text{corr}}(|\psi|^2) + \varepsilon_1(n) \right]. \quad (1.24)$$

Notice the presence of the last term  $\varepsilon_1(n)$ , not appearing in Hartree equation Eq. (1.23). We want to verify that this expression can describe the ground state properties of both weakly interacting Bose gases and superfluid helium. At equilibrium, for an untrapped resting fluid,  $V_{\text{ext}} = 0$ ,  $|\psi|^2 \rightarrow n$  and  $\nabla\psi = 0$ . For a weakly-interacting Bose gas both  $\varepsilon_{\text{corr}}(n)$  and  $\varepsilon_1(n)$  are negligible and we get, as expected

$$\frac{E}{V} = \frac{1}{2} g_0 n^2, \quad (1.25)$$

where  $g_0$  is the integral of the interaction potential  $V(\mathbf{r}, \mathbf{r}') = V(|\mathbf{r} - \mathbf{r}'|)$ . In the case of the superfluid helium both  $\varepsilon_{\text{corr}}(n)$  and  $\varepsilon_1(n)$  are relevant, and we have

$$\frac{E}{V} = \frac{1}{2} g_0 n^2 + \varepsilon_{\text{corr}}(n) + \varepsilon_1(n). \quad (1.26)$$

It is evident that we can always properly choose  $\varepsilon_{\text{corr}}$  and  $\varepsilon_1$  to reproduce the experimental equation of state as reported in [19]:

$$\frac{E}{V} = -\frac{V_0}{2} n^2 - \frac{V_1}{3} n^3 + \frac{V_2}{4} n^4, \quad (1.27)$$

where  $V_0 = 719 k_B \text{ \AA}^3 \text{ K}$ ,  $V_1 = 3.63 \cdot 10^4 k_B \text{ \AA}^6 \text{ K}$  and  $V_2 = 2.48 \cdot 10^6 k_B \text{ \AA}^9$ .

### 1.3 Scattering theory and finite range approximation

With regards to dilute ultra-cold Bose gases, in many cases it is useful to improve the GP model overcoming the simple zero-range approximation for the interaction potential between bosons and extending it to a finite-range model, [20], [21]. Hence we want to introduce a correction term to the potential Eq. (1.1) to obtain a modified Gross-Pitaevskii

equation. Firstly we hypotize that the interaction potential  $V$  between bosons pairs depends only on the interparticle distance  $r = |\mathbf{r}| = |\mathbf{r} - \mathbf{r}'|$ :

$$V(r) = V(|\mathbf{r} - \mathbf{r}'|).$$

Now we analyze this potential in momentum space: for weakly interacting Bose gases BEC is a phenomenon that occurs in momentum space and, in low energy approximation, it consists in a macroscopic occupation of quantum state  $\mathbf{q} = 0$ . So we can study our mean-field potential  $U_{\text{mf}}$

$$U_{\text{mf}} = \int d^3\mathbf{r}' V(|\mathbf{r} - \mathbf{r}'|) |\psi(\mathbf{r}', t)|^2$$

making a Fourier transform<sup>1</sup>. Remembering that the Fourier transform of a convolution is the product of the convoluted terms' transforms, under proper hypotesis of analyticity for them, we obtain

$$\mathcal{F}[U_{\text{mf}}](\mathbf{q}) = \mathcal{F} \left[ \int d^3\mathbf{r}' V(|\mathbf{r} - \mathbf{r}'|) |\psi(\mathbf{r}', t)|^2 \right] (\mathbf{q}) = \mathcal{F}[V(r)](\mathbf{q}) \mathcal{F}[|\psi|^2](\mathbf{q}). \quad (1.28)$$

Now we can expand the term  $\hat{V}(\mathbf{q}) = \mathcal{F}[V(r)](\mathbf{q})$  in MacLaurin series, because the most relevant contribute is around  $\mathbf{q} = 0$ . Since  $V(r)$  is a radial function, hence invariant for parity in coordinates space, its transform conserves the same simmetry property in momentum space and so its MacLaurin expansion contains only even terms. If the expansion is truncated at the second order we have

$$\hat{V}(\mathbf{q}) = \sum_{n=0}^{\infty} \frac{\hat{V}^{(2n)}(0)}{(2n)!} q^{2n} = \hat{V}(0) + \frac{1}{2} \hat{V}''(0) q^2 + \mathcal{O}(q^4).$$

Substituting in Eq. (1.28) and antitransforming with  $\mathcal{F}[\nabla f](\mathbf{q}) = i\mathbf{q}\hat{f}(\mathbf{q})$  we have

$$U_{\text{mf}} = \left[ \hat{V}(0) - \frac{1}{2} \hat{V}''(0) \nabla^2 \right] |\psi(\mathbf{r}, t)|^2. \quad (1.29)$$

We define the constants

$$g_0 = \hat{V}(0) = \int d^3\mathbf{r} V(r), \quad g_2 = \frac{1}{2} \hat{V}''(0) = -\frac{1}{6} \int d^3\mathbf{r} r^2 V(r).$$

So in momentum space we can choose a pseudopotential of the form

$$\hat{V}(q) = g_0 + g_2 q^2, \quad (1.30)$$

corresponding, as proved in [20], to a pseudopotential in real space of the form

$$V(r) = g_0 \delta(r) - \frac{g_2}{2} \left[ \overleftarrow{\nabla}^2 \delta(r) + \overrightarrow{\nabla}^2 \delta(r) \right]. \quad (1.31)$$

Substituting this potential in Eq. (1.23) under the same hypotesis of the GPE we obtain the modified Gross-Pitaevskii equation (MGPE)

$$i\hbar \frac{\partial}{\partial t} \psi(\mathbf{r}, t) = \left[ -\frac{\hbar^2}{2m} \nabla^2 + V_{\text{ext}}(\mathbf{r}) + g_0 |\psi(\mathbf{r}, t)|^2 - g_2 \nabla^2 |\psi(\mathbf{r}, t)|^2 \right] \psi(\mathbf{r}, t). \quad (1.32)$$

We want now to study in detail, with the help of scattering theory, the parameters  $g_0$  and  $g_2$  for ultra-cold gases. The scattering process between two identical particles is described

<sup>1</sup>The Fourier transform of a function  $f(x)$  is defined as

$$\hat{f}(k) = \mathcal{F}[f(x)](k) = \int_{-\infty}^{\infty} dx f(x) e^{-ikx}.$$

by a wave function  $\phi(\mathbf{r})$  depending on the relative coordinate  $\mathbf{r}$ ; it is the overlap of an incident plane wave function and a diffuse spherical wave function. Let  $\mathbf{q}$  and  $\mathbf{q}'$  be the incident particle's and the diffuse particle's momenta, respectively. We have

$$\phi(\mathbf{r}) = e^{i\mathbf{q}\cdot\mathbf{r}} + f(\mathbf{q}, \mathbf{q}') \frac{e^{iqr}}{r}.$$

The function  $f(\mathbf{q}, \mathbf{q}')$  is called scattering amplitude and its analytical expression can be found as a function of the pair interaction potential  $V(|\mathbf{r} - \mathbf{r}'|)$  solving the stationary Schrödinger equation for the scattering process. If the interaction potential is negligible beyond a characteristic range  $r_0$  (Born approximation), we can compute the scattering amplitude using free particle wave functions. So we have

$$\text{Re}[f(\mathbf{q}, \mathbf{q}')] \simeq -\frac{m}{4\pi\hbar^2} \int d^3\mathbf{r} V(\mathbf{r}) e^{-i(\mathbf{q}-\mathbf{q}')\cdot\mathbf{r}} = -\frac{m}{4\pi\hbar^2} \hat{V}(\mathbf{q} - \mathbf{q}'). \quad (1.33)$$

From Eq. (1.33) the close link between the Fourier transform of the interaction potential and the scattering amplitude is clear. The diffused spherical wave can be seen as a combination of partial waves characterized by different values of angular momentum  $\ell$ : they are called s-waves for  $\ell = 0$ , p-waves for  $\ell = 1$  and so on. Hence we can expand the scattering amplitude in partial waves  $f_\ell(q)$  depending on the values of angular momentum. Considering also the incident plane wave as a combination of spherical waves, it can be proved [22] that the presence of the interaction potential implies the variation of the single diffused spherical wave function by a coefficient  $1 + 2iqf_\ell(q) = e^{2i\delta_\ell(q)}$ , in which  $\delta_\ell(q)$  is called phase-shift of the partial wave  $f_\ell(q)$ . Now we can write the scattering cross section as a function of the incident particle's momentum and expand in series over all components of the incident wave

$$\sigma(q) = \sum_{\ell=0}^{\infty} \frac{4\pi}{q^2} (2\ell + 1) \sin^2 \delta_\ell(q).$$

Since particles at low temperatures have not enough energy to access levels of higher angular momenta, for ultra-cold gases the leading term is the one determined by the s-wave:

$$f(\mathbf{q}, \mathbf{q}') \simeq f_0(q) = \frac{e^{2i\delta_0(q)} - 1}{2iq} = \frac{e^{i\delta_0(q)}}{q} \sin \delta_0(q).$$

Computing the cross section in the s-wave limit we obtain

$$\lim_{q \rightarrow 0} \sigma(q) = 4\pi \frac{\sin^2 \delta_0(q)}{q^2} = 4\pi a_s^2,$$

where we defined the s-wave scattering length  $a_s$ , a quantity used in atomic physics to characterize the interactions between atoms in the low energy limit

$$a_s = -\lim_{q \rightarrow 0} \frac{\sin \delta_0(q)}{q}, \quad (1.34)$$

and the effective range  $r_e$  as the quadratic coefficient of the following expansion (see for example [22])

$$q \cot(\delta_0(q)) = -\frac{1}{a_s} + \frac{1}{2} r_e q^2 + \mathcal{O}(q^4). \quad (1.35)$$

Considering the real part of the scattering amplitude and expanding in MacLaurin series for  $q$  we find

$$\begin{aligned} \text{Re}[f_0(q)] &= \frac{1}{2q} \sin(2\delta_0(q)) = q \cot \delta_0(q) \frac{\sin^2 \delta_0(q)}{q^2} \\ &= \left( -\frac{1}{a_s} + \frac{1}{2} r_e q^2 + \mathcal{O}(q^4) \right) \left( + a_s^2 + a_s^3 q^2 (r_e - a_s)^2 + \mathcal{O}(q^4) \right). \end{aligned} \quad (1.36)$$

So, comparing Eq. (1.36) and Eq. (1.33), we have

$$\hat{V}(q) = -\frac{4\pi\hbar^2}{m} \left[ -a_s + \left( a_s - \frac{1}{2}r_e \right) a_s^2 q^2 + \mathcal{O}(q^4) \right], \quad (1.37)$$

from whom expressions for  $g_0$  e  $g_2$  can be found, in agreement with [20]

$$g_0 = \hat{V}(0) = \frac{4\pi\hbar^2}{m} a_s, \quad (1.38)$$

$$g_2 = \frac{1}{2} \hat{V}''(0) = \frac{4\pi\hbar^2}{m} \left( \frac{1}{2}r_e - a_s \right) a_s^2.$$

Let us also point out that the sign of the parameters depends on the interatomic potential: for  $a_s > 0$  the interaction is repulsive at low momenta, if  $a_s < 0$  is attractive. The two parameters  $a_s$  and  $r_e$  are generally related depending on the analytical form of the interaction potential. For example, for a hard-sphere potential with radius  $a_s$ , we have the relation.

$$r_e = \frac{2}{3} a_s. \quad (1.39)$$

## 2

# Elementary excitations

In this chapter we will study, with the formalism developed above, the excitation spectrum of bosonic superfluids. In the first section, with the help of Landau's theory, we will see the reasons why we can say that ultra-cold Bose gases and  $^4\text{He}$  show superfluid properties. In the second section we will focus on elementary excitation in bosonic superfluid and we will find the form of the dispersion relation from the Hartree equation or the MGPE. Then, in the last section, we will employ those relations to describe the spectra of a BEC and of superfluid  $^4\text{He}$  and we will compare the results with experimental data.

## 2.1 Superfluid behavior and Landau's criterion

Let us consider for simplicity an ultra-cold Bose gas described by the MGPE: similar considerations can be done for  $^4\text{He}$ . Since the superfluid fraction of particle corresponds to the condensate one, we can write the order parameter as a single particle wave function using the Madelung transform:

$$\psi(\mathbf{r}, t) = \sqrt{n(\mathbf{r}, t)} e^{i\theta(\mathbf{r}, t)}. \quad (2.1)$$

The superflow arises when the phase  $\theta$  varies in space [16]. Employing the usual quantum mechanics' formula with the wave function just defined, we can write the current density

$$\mathbf{j}(\mathbf{r}, t) = \frac{\hbar}{2mi} [\psi^* \nabla \psi - \psi \nabla \psi^*] = \frac{\hbar}{m} n(\mathbf{r}, t) \nabla \theta(\mathbf{r}, t). \quad (2.2)$$

Since  $\mathbf{j}(\mathbf{r}, t) = n(\mathbf{r}, t) \mathbf{v}(\mathbf{r}, t)$  we obtain the fundamental relation for the superfluid velocity

$$\mathbf{v}(\mathbf{r}, t) = \frac{\hbar}{m} \nabla \theta(\mathbf{r}, t). \quad (2.3)$$

This relation, along with the Madelung transform, leads to a fluid dynamics interpretation of the ultra-cold Bose gas [24]. In fact, substituting Eq. (2.1) in the MGPE Eq. (1.32) and equating the real and the imaginary part of each member, we obtain two equations: a continuity equation and a dynamic one:

$$\frac{\partial n}{\partial t} + \nabla \cdot (n \mathbf{v}) = 0, \quad (2.4)$$

$$mn \frac{\partial \mathbf{v}}{\partial t} + \nabla \left[ -\frac{\hbar^2}{2m} \sqrt{n} \nabla^2 \sqrt{n} + \frac{1}{2} mn v^2 + V_{\text{ext}} n + g_0 n^2 - g_2 n \nabla^2 n \right] = 0. \quad (2.5)$$

The first term in brackets  $\mathcal{P} = -\frac{\hbar^2}{2m} \sqrt{n} \nabla^2 \sqrt{n}$  is called quantum pressure while the last terms are proportional to the equation of state of the system. Eq. (2.4) and Eq. (2.5)

are called *superfluid hydrodynamics equations* and, except for the quantum pressure term and the finite range, are similar to Euler equations for an irrotational fluid (note that  $\nabla \times \mathbf{v} = 0$ ) and with zero viscosity.

We can simply estimate the importance of the quantum pressure term, the finite range term and the GP model equation of state  $P_0 = \frac{1}{2}g_0n^2$  introducing a characteristic length  $\xi$  representing the length at which density changes occur in the condensate:  $\nabla^2 n \simeq n/\xi^2$ . So

$$\frac{\mathcal{P}}{P_0} \simeq \frac{\hbar^2}{2g_0nm\xi^2}.$$

Hence  $\mathcal{P} \ll P$  in the limit of  $\lambda \ll \xi$ : in this regime and for a zero external potential the Eq. (2.4) and Eq. (2.5) reduce to the Euler equations for zero viscosity. Neglecting finite-range interactions  $g_2 = 0$  we define the *healing length* as

$$\xi = \sqrt{\frac{\hbar^2}{2g_0nm}}. \quad (2.6)$$

If  $g_2 \neq 0$  we can define a new healing length, equaling the kinetic term and potential term in the MGPE equation Eq. (1.32). Remembering that  $|\psi|^2 \propto n$  and  $\nabla^2 n \simeq n/\xi'^2$  the healing length for the MGPE  $\xi'$  is given by  $\xi' = \xi\sqrt{1-\alpha}$ , where  $\alpha$  is an adimensional parameter

$$\alpha = -\frac{g_2}{g_0\xi^2}. \quad (2.7)$$

So, if we consider finite-range interactions, the healing length of the system will change in magnitude accordingly to the sign of the parameter  $\alpha$  depending itself on the sign of  $g_0$  and  $g_2$ . This ideas will be useful to study quantized vortices in weakly interacting Bose gases, as we shall see in section 3.2.

Now we want to show that both dilute ultra-cold Bose gases and He II, described by the MGPE and Hartree equation respectively, have a superfluid behavior, i.e. they flow without friction. We will use a simple criterion developed by Landau [23], [16], [24] that employs Galilean invariance. Let us first consider a fluid of mass  $M$  at absolute zero flowing along a capillary at a constant velocity  $\mathbf{v}$ . For an ordinary fluid viscosity and dissipation arise when the flowing fluid particles are randomly scattered by the atoms of the channel's walls, so we have momentum transfer from the fluid to the walls: if viscosity is zero it means that this scattering events do not occur. Let us consider the system in the frame in which the fluid is at rest and the walls move with velocity  $-\mathbf{v}$ . When viscosity is present the fluid also begins to move: it is clear that the motion must arise gradually as elementary excitations in the fluid appear. Let us suppose a single elementary excitation of momentum  $\mathbf{q}$  and energy  $\hbar\omega(\mathbf{q})$  arising in the fluid: so, since we are considering the fluid at rest, its energy  $E$  and momentum  $\mathbf{p}$  are equal to  $\hbar\omega(\mathbf{q})$  and  $\hbar\mathbf{q}$ . We will regard the excitation as a quasiparticle. If we now consider the frame in which the walls are at rest, thanks to Galilean transformation  $\mathbf{p}' = \mathbf{p} + M\mathbf{v}$ , we find

$$E' = \frac{\mathbf{p}'^2}{2M} = E + \mathbf{p} \cdot \mathbf{v} + \frac{1}{2}Mv^2, \quad (2.8)$$

and substituting the values for  $E(\mathbf{q}) = \hbar\omega(\mathbf{q})$  and  $\mathbf{p}$  we obtain

$$E' = \hbar\omega(\mathbf{q}) + \hbar\mathbf{q} \cdot \mathbf{v} + \frac{1}{2}Mv^2. \quad (2.9)$$

Since  $\frac{1}{2}Mv^2$  is the kinetic energy of the flow, the change in energy is given by  $E(\mathbf{q}) + \hbar\mathbf{q} \cdot \mathbf{v}$  which must be negative since friction decreases the energy of the fluid. The quantity  $\hbar\mathbf{q} \cdot \mathbf{v}$  is at minimum when the excitation occurs in a direction antiparallel to flow, so we must always have  $E(q) - \hbar qv < 0$ , i.e.

$$v > v_L = \min_q \frac{E(q)}{\hbar q}, \quad (2.10)$$



which is the so-called Landau's criterion for superfluidity. The condition for the occurrence of excitations and so for non-zero viscosity is given finding the minimum of  $E(q)/\hbar q$ , i.e. geometrically the minimum slope  $v_L$  of the line drawn from the origin to each point of an excitation spectrum in a  $(q, E(q))$  graph. If the critical Landau velocity  $v_L$  is not zero, then, for velocities of flow below a certain value, excitations cannot appear in the fluid and so the system shows the phenomenon of superfluidity. To find if this criterion is satisfied by ultra-cold Bose gases and He II we have to find the expression of  $E(q)$ .

## 2.2 Quasiparticle dispersion relation

In this section we will obtain the dispersion relation in a general form for both weakly interacting gases and  $^4\text{He}$ . Let us start considering Hartree equation Eq. (1.23) with  $V_{\text{ext}} = 0$ . The dispersion relation can be obtained in the case of an homogeneous and infinitely extended fluid: the solution at equilibrium is constant  $\psi = \psi_0$  and corresponds to a constant density profile. At infinity we obtain the relation

$$\mu = \int d^3\mathbf{r}' V(|\mathbf{r} - \mathbf{r}'|) |\psi_0|^2 + \mu_{\text{corr}}(|\psi_0|^2), \quad (2.11)$$

which can also be written as

$$\mu = g_0 |\psi_0|^2 + \mu_{\text{corr}}(|\psi_0|^2). \quad (2.12)$$

Let us now consider a small perturbation  $\eta(\mathbf{r}, t)$

$$\psi(\mathbf{r}, t) = \left[ \psi_0 + \eta(\mathbf{r}, t) \right] e^{-i\mu t/\hbar}. \quad (2.13)$$

Substituting in Eq. (1.23) and keeping only first order terms in  $\eta$  and  $\eta^*$ , we get these terms (we omit the phase term  $e^{-i\mu t/\hbar}$ )

$$\begin{aligned} i\hbar \frac{\partial \psi}{\partial t} &= \left[ i\hbar \frac{\partial \eta}{\partial t} + \mu(\psi_0 + \eta) \right]. \\ \psi \int d^3\mathbf{r}' V(r') |\psi|^2 &= (\psi_0 + \eta) \int d^3\mathbf{r}' V(r') \left[ |\psi_0|^2 + \psi_0(\eta + \eta^*) \right] \\ &= g_0 |\psi_0|^2 (\psi_0 + \eta) + |\psi_0|^2 \int d^3\mathbf{r}' V(r') (\eta + \eta^*). \\ \psi \mu_{\text{corr}}(|\psi|^2) &= (\psi_0 + \eta) \left[ \mu_{\text{corr}}(|\psi_0|^2) + \psi_0(\eta + \eta^*) \frac{\partial \mu_{\text{corr}}(|\psi_0|^2)}{\partial |\psi_0|^2} \right] \\ &= \mu_{\text{corr}}(|\psi_0|^2) (\psi_0 + \eta) + |\psi_0|^2 \frac{\partial \mu_{\text{corr}}(|\psi_0|^2)}{\partial |\psi_0|^2} (\eta + \eta^*). \end{aligned}$$

Now using Eq. (2.12) we obtain the following differential equation:

$$i\hbar \frac{\partial \eta}{\partial t} = \frac{\hbar^2}{2m} \nabla^2 \eta + |\psi_0|^2 \int d^3\mathbf{r}' V(r') [\eta + \eta^*] + |\psi_0|^2 \frac{\partial \mu_{\text{corr}}(|\psi_0|^2)}{\partial |\psi_0|^2} [\eta + \eta^*]. \quad (2.14)$$

Regarding  $|\psi_0|^2$  as the particle density in unit volume  $n$  we can write Eq. (2.14) as

$$i\hbar \frac{\partial \eta}{\partial t} = \frac{\hbar^2}{2m} \nabla^2 \eta + n \int d^3\mathbf{r}' V(r') [\eta + \eta^*] + n \frac{\partial \mu_{\text{corr}}}{\partial n} [\eta + \eta^*]. \quad (2.15)$$

Considering perturbations in the form of plane waves of frequency  $\omega$  and wave vector  $\mathbf{q}$

$$\eta(\mathbf{r}, t) = A e^{i(\mathbf{q}\cdot\mathbf{r} - \omega t)} + B^* e^{-i(\mathbf{q}\cdot\mathbf{r} - \omega t)},$$

and substituting in Eq. (2.15) we obtain a system of equations in  $A$  e  $B$ :

$$\begin{aligned} \left[ -\hbar\omega + \frac{\hbar^2 q^2}{2m} + n\hat{V}(q) + n\frac{\partial\mu_{\text{corr}}}{\partial n} \right] A + \left[ n\hat{V}(q) + n\frac{\partial\mu_{\text{corr}}}{\partial n} \right] B &= 0 \\ \left[ n\hat{V}(q) + n\frac{\partial\mu_{\text{corr}}}{\partial n} \right] A + \left[ +\hbar\omega + \frac{\hbar^2 q^2}{2m} + n\hat{V}(q) + n\frac{\partial\mu_{\text{corr}}}{\partial n} \right] B &= 0 \end{aligned}$$

which has non-trivial solution if and only if

$$E(q) = \sqrt{\frac{\hbar^2 q^2}{2m} \left\{ \frac{\hbar^2 q^2}{2m} + 2n \left[ \hat{V}(q) + \frac{\partial\mu_{\text{corr}}}{\partial n} \right] \right\}}. \quad (2.16)$$

If this relation is monotonic, the critical Landau velocity is equal to the first sound velocity we get from expanding Eq. (2.16) at first order in  $q$

$$c = \lim_{q \rightarrow 0} \frac{1}{q\hbar} E(q) = \sqrt{\frac{n}{m} \left[ \hat{V}(0) + \frac{\partial\mu_{\text{corr}}}{\partial n} \right]}. \quad (2.17)$$

Let us see what form takes the dispersion relation in case of a weakly interacting Bose gas with finite range interactions. In that case we have  $\mu_{\text{corr}} = 0$ ,  $\mu = g_0 n$  and  $\hat{V}(q) = g_0 + g_2 q^2$ . Hence we get

$$E_{\text{fr}}(q) = \sqrt{\frac{\hbar^2 q^2}{2m} \left\{ \frac{\hbar^2 q^2}{2m} + 2\mu \left[ 1 + \frac{g_2 q^2}{g_0} \right] \right\}}. \quad (2.18)$$

Note that for  $g_2 = 0$  one obtains the well-known Bogoliubov dispersion relation [24], [25] and from it the sound velocity

$$c = \sqrt{\frac{\mu}{m}}. \quad (2.19)$$

The expansions at low momenta are justified by the low temperature hypothesis. This is the same as stating that  $q^2 \ll \frac{2\mu m}{\hbar^2} = 1/\xi^2$  i.e.  $1/q^2 \sim \lambda^2 \gg \xi^2$  hence we have a length scale also for phenomena in momentum space. Notice that in absence of interaction  $g_0 = 0$ ,  $\mu = g_0 n = 0$  and the critical velocity is zero. Hence a non-interacting BEC is not a superfluid.

## 2.3 Excitation spectrum for a weakly-interacting Bose gas

The elementary excitation spectrum of an ultra-cold alkali gas is monotonic with a shape that resembles the free particle spectrum. We want to compare the dispersion curve obtained from Eq. (2.18) with experimental data obtained by the group of Davidson [26]. They considered a BEC of  $^{87}\text{Rb}$  atoms in the  $5s_{1/2}$ ,  $F = 2$ ,  $m_F = 2$ , trapped by a magnetic field and cooled with an evaporation technique similar to the one described in section 1.1. Our Eq. (2.18) has been found for homogeneous condensate but, as stated by the authors, the dispersion curve of the trapped condensate should largely reflect the intrinsic properties of the homogeneous BEC. If we set  $\xi = \sqrt{\frac{\hbar^2}{2\mu m}}$  and  $2\mu = \frac{\hbar^2}{m\xi^2}$  as unit of length and energy respectively, with  $\mu/h = 1.91$  kHz the measured chemical potential, we can write Eq. (2.18) in the form:

$$\omega_{\text{fr}}(q) = \frac{\hbar}{m\xi^2} \sqrt{\frac{q^2 \xi^2}{2} \left\{ \frac{q^2 \xi^2}{2} + \left[ 1 - \alpha q^2 \xi^2 \right] \right\}}. \quad (2.20)$$

with  $\alpha = -g_2 \xi^{-2}/g_0$ , the adimensional parameter defined in Eq. (2.7). In the case of  $^{87}\text{Rb}$  the scattering length is  $a_s = 90.6a_0 \simeq 48 \text{ \AA}$  [9] and from this value we can compute  $g_2$

once we know  $\alpha$ . To see if our model suits the data we tried to fit them with Eq. (2.20) with free parameter  $\alpha$ . In Fig. (2.1) we show the experimental data together with our fit, the spectrum obtained with the GPE model ( $\alpha = 0$ ) and the free particle curve  $\omega_0 = \frac{\hbar q^2}{2m}$ . From the fit we obtained the value  $\alpha \simeq 0.08$ . We see that our model improves the GP one at medium and short wavelengths but lacks accuracy at low momenta, i.e. in the so-called phonon part of the spectrum, due to other effects not taken in account by our simple model and to the fact that the atoms are trapped. The authors in [26] employed an improved Bogoliubov spectrum in the local density approximation (LDA) in which the speed of sound  $c_{ld}(q)$  is not constant like in the MGPE model but slowly varies:

$$c_{ld}(q) = \frac{\hbar q}{2m} \sqrt{S(q)^{-2} - 1}, \quad (2.21)$$

where  $S(q)$  is the structure factor giving the magnitude of density fluctuations in the fluid. The authors considered the following form with  $\Theta = 2\mu/(\hbar\omega_0(q))$  adimensional function of momentum

$$S(q) = \frac{15}{4} \left\{ \frac{3 + \Theta}{4\Theta^2} - \frac{3 + 2\Theta - \Theta^2}{16\Theta^{5/2}} \left[ \pi + 2 \arctan \left( \frac{\Theta - 1}{2\sqrt{\Theta}} \right) \right] \right\}. \quad (2.22)$$

So the dispersion relation that fits the data is

$$\omega_{ld}(q) = \sqrt{\left(\frac{\hbar q^2}{2m}\right)^2 + c_{ld}^2(q)q^2}. \quad (2.23)$$

From this model the speed of sound, which is also the Landau critical velocity, is  $c_{\text{eff}} = \frac{32}{15\pi} \sqrt{\frac{\mu}{m}} \simeq 0.68c$ , a little smaller than our speed of sound.

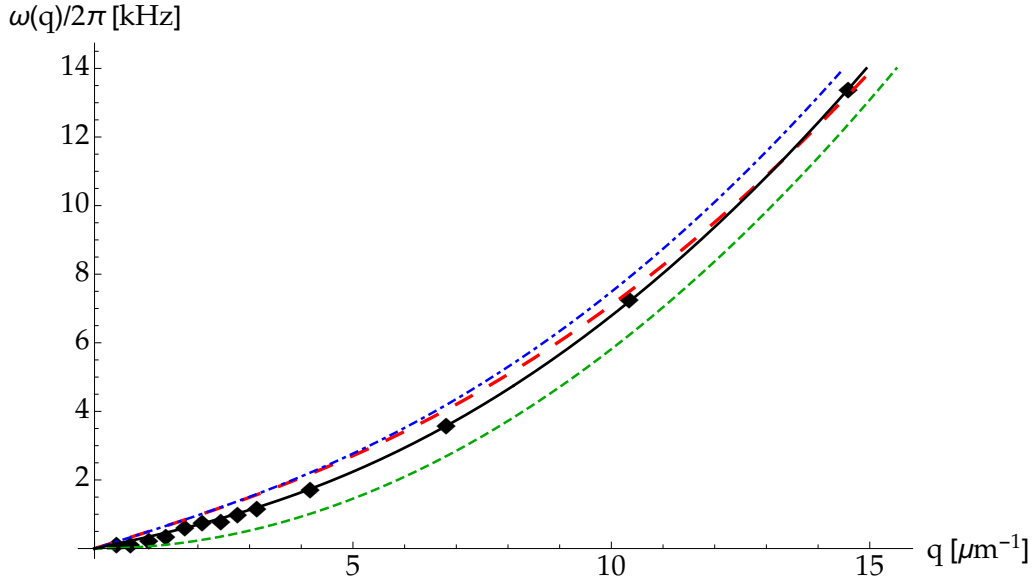


Figure 2.1: The elementary excitation spectrum for a  $^{87}\text{Rb}$  BEC: " $\diamond$ " data from [26], the fit dispersion curve from Eq. (2.20) for  $\alpha \simeq 0.08$  (large-dashed red line), the GP model dispersion curve (dot-dashed blue line), the LDA dispersion curve Eq. (2.23) (solid black line) and the free particle spectrum  $\omega_0$  (short-dashed green line).

## 2.4 Excitation spectrum for superfluid ${}^4\text{He}$

Let us consider liquid helium at zero temperature and pressure. The elementary excitation spectrum for liquid helium obtained via experiments, e.g. with neutron scattering methods (see the works of Donnelly [27]), is not monotonic but has a characteristic trend. There are three main regions in the spectrum. At very low momenta  $q$  the energy is, as expected, approximately linear  $E(q) = \hbar c q$  with  $c = 238$  m/s: such behaviour is similar to quasiparticle excitations called *phonons* in solid state physics. This region corresponds to greater  $\lambda_{\text{dB}}$  than a single atom size and is due to a rigid movement of groups of atoms together. At higher values of momenta we have a minimum, called the *roton* part of the spectrum in which the energy goes as

$$E(q) = \Delta + \frac{\hbar^2}{2m^*}(q - q_0)^2, \quad (2.24)$$

with extrapolated parameters  $m^* = 0.16 m_{{}^4\text{He}}$ ,  $\Delta = 8.7$  K and  $q_0 = 1.926 \text{ \AA}^{-1}$ . It is worth saying that this form of the spectrum was first suggested by Landau (1947) from an analysis of experimental results regarding the thermodynamic quantities for liquid helium and only later confirmed by neutron scattering experiments. In the roton region  $\lambda_{\text{dB}}$  is of the order of the interparticle distance  $n^{-1/3}$  so the moving particle couples strongly to the surrounding ones leading to a circular motion around the travelling particle. We will see that the roton part of the spectrum is the most important one and it affects the profile of quantized vortices in  ${}^4\text{He}$ . In conclusion, at even higher momenta, the experimental spectrum shows a saturation rather than a conventional free-particle one. According to [14], [13], we will ignore this feature, assuming at high momenta a similar to free-particle spectrum.

Now we want to reproduce the experimental spectrum of  ${}^4\text{He}$  using Eq. (2.16): so we have to choose the analytic form of  $\mu_{\text{corr}}$  and of the potential  $V(r)$ . Following the work of Berloff [14] [28] and Dalfovo [13], [12], we choose the correlation term  $\mu_{\text{corr}}$  as follows

$$\mu_{\text{corr}} = W|\psi|^{2(1+\nu)}, \quad (2.25)$$

in analogy with Skyrme correlation energy adopted for atomic nuclei [18], with  $W$  and  $\nu$  as free parameters. As proved in [29] this term is necessary, otherwise the model would have non-physical features such as non-dissipative mass concentrations. For the two-body interaction potential  $V(|\mathbf{r} - \mathbf{r}'|)$ , following again Berloff and Jones [14], [28] we chose

$$V(r) = V_0 \left[ (\alpha + \beta r^2 A^2 + \gamma r^4 A^4) e^{-A^2 r^2} + \delta e^{-B^2 r^2} \right] \quad (2.26)$$

with the constant  $V_0$ , dimensionally an energy, and the parameters  $A$ ,  $B$ ,  $\alpha$ ,  $\beta$ ,  $\gamma$ ,  $\delta$ . This choice allows us to work with a Fourier-transformable potential without the need of screening a more realistic 12-6 Lennard-Jones potential [12] at little values of  $r$ . It is important to state that the resulting potential is not a completely realistic interaction potential for liquid helium but it is meant to embody other correlation effects. We chose the values of the parameters with requirements: (1) the dispersion relation obtained by substituting this potential in Eq. (2.16) gives a good fit to experimental data for the phonon and roton part of the spectrum, (2) the normalization condition at infinity is satisfied, (3) the two-body interaction shows a strong repulsion at short distances, (4) the parameters lead to a s-wave scattering length  $a_s$  computed from this potential  $V(r)$  equal to the helium experimental one  $a_s = 2.2 \text{ \AA}$  (see [30] and references therein); as we shall see, this sets a constraint for parameters  $W$  and  $\nu$ . The Fourier transform of Eq. (2.26) reads

$$\hat{V}(q) = \frac{1}{16} \pi^{3/2} V_0 \left\{ \frac{e^{-\frac{q^2}{4A^2}}}{A^3} \left[ 16\alpha + 4\beta \left( 6 - \frac{q^2}{A^2} \right) + \gamma \left( 60 - \frac{20q^2}{A^2} + \frac{q^4}{A^4} \right) \right] + 16\delta \frac{e^{-\frac{q^2}{4B^2}}}{B^3} \right\}.$$

We set  $\xi = \sqrt{\frac{\hbar^2}{2\mu m}}$  and  $2\mu = \frac{\hbar^2}{m\xi^2}$  as unit of length and energy of our model respectively. Then we notice that in Eq. (2.16) the term with  $\mu_{\text{corr}}$  becomes  $2n\frac{\partial\mu_{\text{corr}}}{\partial n} = 2(1+\nu)Wn^{1+\nu}$ , which is an energy. So we set the dimensionless parameter

$$\chi = \frac{Wn^{1+\nu}}{\mu}, \quad (2.27)$$

and  $V_0 = \mu\xi^{-3}/n$ . We can write the dispersion relation for our model in the form

$$E(q) = \frac{\hbar^2}{m\xi^2} \sqrt{\frac{q^2\xi^2}{2} \left\{ \frac{q^2\xi^2}{2} + \left[ \hat{V}(\xi q) + (1+\nu)\chi \right] \right\}}. \quad (2.28)$$

Requesting the bulk normalization Eq. (2.12) we get the constraint for  $\chi$  and for the fit parameters

$$\chi = 1 - \hat{V}(0). \quad (2.29)$$

This also sets the speed of sound of the model from Eq. (2.28) as  $c = \frac{\hbar^2}{m\xi^2} \sqrt{\frac{1+\chi\nu}{2}}$ . Since we know the experimental speed of sound  $c$  we can obtain the expression for the healing length of the model:

$$\xi = \frac{\hbar}{\sqrt{2}mc} \sqrt{1+\chi\nu} \simeq 0.471 \sqrt{1+\chi\nu} \text{ \AA}. \quad (2.30)$$

Now we can explicit the constraint on the scattering length

$$a_s = \frac{m\hat{V}(0)}{4\pi\hbar^2} = \frac{\sqrt{2}mc}{n\hbar} \cdot \frac{1-\chi}{\sqrt{1+\nu\chi}}. \quad (2.31)$$

This shows that once we set the value of  $\nu$ , Eq. (2.31) fixes the value of  $\chi$ , hence the healing length of the model  $\xi$ . More freedom can be obtained relaxing the requirement (4). We chose  $\nu = 1$  and we obtained from Eq. (2.31) the value of  $\chi \simeq 0.58$ . From the fit with Eq. (2.28) shown in Fig. (2.2) we obtained the values of the parameters  $A \simeq 1.9$ ,  $\alpha \simeq 4.833$ ,  $\beta \simeq -2.602$ ,  $\gamma \simeq -1.822$ ,  $B \simeq 0.567$  and  $\delta \simeq 0.171$ . In Fig. (2.2) we also show how the finite range approximation of the potential Eq. (2.26,  $E_{\text{fit}}$ ), can well reproduce the data for the phonon part of the spectrum, the critical velocity  $v_L \simeq 56.5$  m/s, close to the experimental one (we must take into account that vortex production lowers the critical velocity [6]), and sound velocity  $c = 238$  m/s. Another possible choice was  $\nu = 2.8$  as it takes into account the right proportionality to the density  $n$  of the sound velocity:  $c \propto n^{2.8}$  as showed by Donnelly and Berloff in [14] and references therein. The result fit is visually identical to the one with  $\nu = 1$  but we obviously obtained different parameters:  $\chi \simeq 0.419$ ,  $A \simeq 1.82$ ,  $\alpha \simeq 10.2$ ,  $\beta \simeq -16$ ,  $\gamma \simeq 1.764$ ,  $B \simeq 0.667$ ,  $\delta \simeq 0.383$ . These fit parameters for  $\nu = 1$  and  $\nu = 2.8$  will be used in section 3.3 to find the density profile of a vortex line in  $^4\text{He}$ .

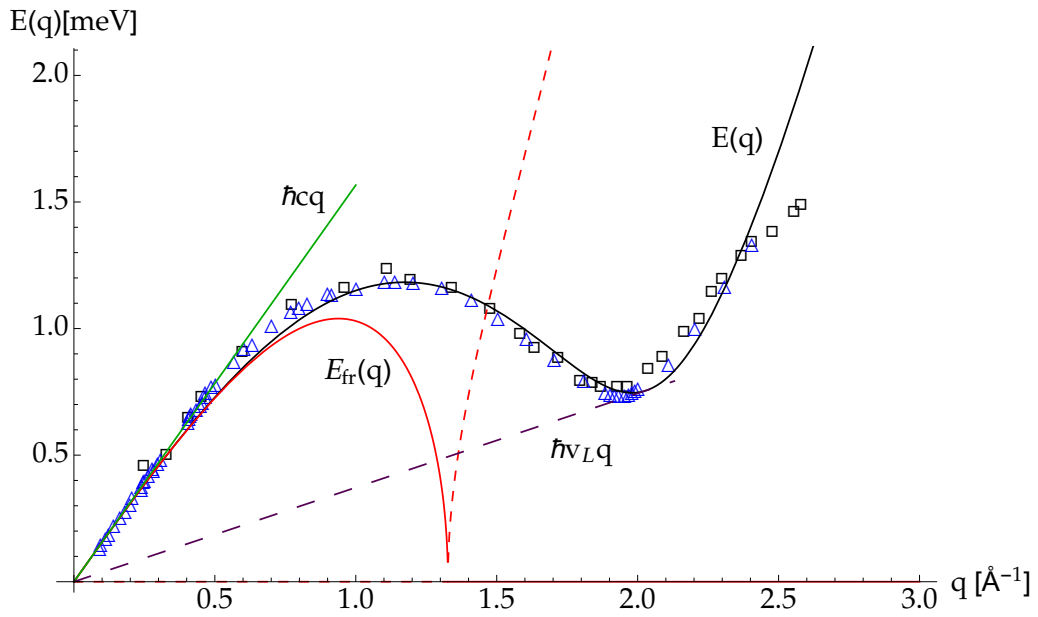


Figure 2.2: The elementary excitation spectrum of  ${}^4\text{He}$ : " $\square$ " data from Annett [16], " $\triangle$ " data from Donnelly [27], the fit  $E(q)$  with Eq. (2.28) for  $\nu = 1$  (solid black line), the real and imaginary part of the finite range approximation  $E_{fr}(q)$  (solid and dashed red lines), sound and critical Landau velocities (solid green and purple long-dashed lines respectively).

# 3

## Quantized vortices

In this chapter we will study the rotational motion in superfluids and particularly the fact that circulation is quantized. In the first section we will obtain the rotational motion quantization from the macroscopic wave function hypothesis and we will study the formation of vortices in a rotating superfluid. In the second section we will solve the stationary MGPE in a particular case for a weakly interacting Bose gas to find the vortex line profile. In conclusion, in the third section, we will solve the complete stationary Hartree equation for He II with the terms obtained in section 2.4 and we will find the vortex line density profile.

### 3.1 Phase defects and vortices

As seen in the first chapter the superfluid can be described by a macroscopic wave function (order parameter) extending over the entire system, written in the form of the Madelung transform Eq. (2.1). We also saw that as a consequence a phase gradient in the system induces an inviscid flow with velocity

$$\mathbf{v}(\mathbf{r}) = \frac{\hbar}{m} \nabla \theta(\mathbf{r}), \quad (3.1)$$

which therefore is also irrotational

$$\nabla \times \mathbf{v} = 0. \quad (3.2)$$

Another important property regards the circulation of the flow. Let us consider a flow around a closed path  $C$  with line element  $d\mathbf{s}$  around a fixed axis  $z$ . If we define the circulation of the flow  $\Gamma$  as

$$\Gamma = \oint_C \mathbf{v} \cdot d\mathbf{s}, \quad (3.3)$$

for the irrotational property the circulation is independent from the choice of the path  $C$  that wraps the axis. Substituting  $\mathbf{v}$  from Eq. (3.1) in Eq. (3.3) we find

$$\Gamma = \oint_C \frac{\hbar}{m} \nabla \theta(\mathbf{r}) \cdot d\mathbf{s} = \frac{\hbar}{m} \Delta \theta. \quad (3.4)$$

But, since the macroscopic wave function  $\psi(\mathbf{r}) = \sqrt{n(\mathbf{r})} e^{i\theta(\mathbf{r})}$  has to be single-valued, it must be  $\Delta \theta = 2\pi s$  where  $s \in \mathbb{Z}$ . This implies that within the considered region there must be a phase defect point, where  $\theta$  takes every value and consistently  $\psi = 0$ : it is a singularity whose presence affects the fluid's properties. First of all the circulation of the flow is quantized:

$$\Gamma = \frac{\hbar s}{m}. \quad (3.5)$$

This is equivalent to imposing the angular momentum quantization  $L = s\hbar$ . Hence the quantized circulation is another property that characterizes flow for superfluids, together with zero viscosity and irrotationality. Introducing cylindrical coordinates  $(r, \theta, z)$ , using Eq. (3.5), and computing the integral in Eq. (3.3) we find the azimuthal speed around the  $z$  axis:

$$v_\theta = \frac{s\hbar}{mr}. \quad (3.6)$$

Eq. (3.6) implies that, to avoid velocity divergence, as  $r \rightarrow 0$  the fluid density, i.e.  $n = |\psi|^2$ , has to be zero. We can now see that a quantized vortex is a well defined topological singularity. The quantum number  $s$  is called vortex charge and it corresponds to the topological winding number of the phase around the closed loop. The flow in a quantized vortex profoundly differs from flow in a classical vortex. To show the main difference let us consider vorticity, a vectorial field defined as  $\boldsymbol{\omega} = \nabla \times \mathbf{v}$  [24]. Unlike the classical case, the irrotational property of the quantum fluid implies that  $\boldsymbol{\omega} = 0$  for  $r > 0$ : therefore a flowing particle will never change its orientation with regards to a reference in the rotational motion. The only contribution to the vorticity is in the singularity itself and it is quantized:  $\boldsymbol{\omega} = \frac{\hbar}{m}\delta^{(3)}(\mathbf{r})\hat{z}$ . Nevertheless, from an experimental point of view, as stated by many authors [6], [10], there are limitations on the definition of the position of the singularity, due to the uncertainty principle. This implies that the vorticity spreads out a little and so we expect a core in which the density becomes very small, but not zero, and the velocity is finite. However, while in classical fluids the vorticity has arbitrary values, in a superfluid the rotational motion around the singularity has well-defined shape and intensity.

Let us give an insight on vortex nucleation. Vortices, as topological defects, can only be created near a boundary or even spontaneously but paired with a vortex of opposite charge. Experimentally they are created by rotating the superfluid, for example in a bucket of radius  $D$ . A vortex is created only if it lowers the energy of the rotating system: this implies that, to create a vortex, the rotational velocity must be greater than a critical value  $\Omega > \Omega_c$ . Since the energy of the vortex is roughly proportional to  $v_\theta^2 \propto s^2$  we can see that multi-charged vortices are less stable than single-charged ones so, if the former are product, they shall decay quite quickly in many single-charged vortices. These vortices arrange themselves in a so-called *vortex lattice*, that have been observed both in  $^4\text{He}$  and in atomic Bose gases [24]. If the necessary critical velocity is exceeded vortices are created near the walls of the bucket and a vortex lattice develops in the bulk, with density increasing with the rotational velocity  $\Omega$ .

To study quantized vortices we will employ the stationary form of our Hartree equation, that we can find substituting

$$\psi(\mathbf{r}, t) = \psi(\mathbf{r})e^{-i\mu t/\hbar}, \quad (3.7)$$

in which  $\mu$  can be easily proved to be the chemical potential. So we find

$$\mu\psi(\mathbf{r}) = \left[ -\frac{\hbar^2}{2m}\nabla^2 + \int d^3\mathbf{r}'V(\mathbf{r}, \mathbf{r}')|\psi(\mathbf{r}')|^2 + \mu_{\text{corr}}(|\psi^2|) \right] \psi(\mathbf{r}). \quad (3.8)$$

## 3.2 Vortices in dilute weakly interacting Bose gases

We want now to study the properties of a vortex in a weakly-interacting Bose gas with singularity in the origin. In dilute atomic BECs the so-called gas parameter  $na_s^3$  is small ( $10^{-4} \div 10^{-8}$ ), therefore the vortex structure can be studied with a local approach, i.e. with the finite range model of the MGPE. Furthermore the diluteness of the gas leads to a large healing length  $\xi \simeq 10^{-6}$  m enabling the experimental observation of the core. We want to concentrate on the effects of the finite range interaction so we will consider an



untrapped BEC of infinite extension and we will employ the stationary MGPE:

$$\left[ -\frac{\hbar^2}{2m} \nabla^2 + g_0 |\psi|^2 - g_2 \nabla^2 |\psi|^2 \right] \psi = \mu \psi. \quad (3.9)$$

The first step is to cast this equation in dimensionless variable. As usual we introduce as unit of length the healing length  $\xi$  defined in Eq. (2.6) and the parameter  $\alpha$  (Eq. (2.7)). Imposing  $\psi \rightarrow \sqrt{n}$  at infinity we fix the chemical potential as  $\mu = g_0 n$ . With the substitutions  $\psi \rightarrow \psi/\sqrt{n}$  and  $\mathbf{r} \rightarrow \xi \mathbf{r}$  we find the dimensionless MGPE:

$$\nabla^2 \psi + \psi - |\psi|^2 \psi - \alpha \nabla^2 |\psi|^2 \psi = 0. \quad (3.10)$$

On the dimensionless coordinates we introduce cylindric coordinates  $(\rho, \theta, \zeta)$  and we write the wave function in the new coordinates to explicit the angular momentum quantization along the  $\zeta$  axis:

$$\psi(\rho, \theta, \zeta) = \phi(\rho) e^{is\theta}, \quad (3.11)$$

with  $s \in \mathbb{Z}$ . Remembering the expression of Laplacian in cylindrical coordinates,

$$\nabla^2 = \frac{1}{\rho} \frac{\partial}{\partial \rho} \left( \rho \frac{\partial}{\partial \rho} \right) + \frac{1}{\rho^2} \frac{\partial^2}{\partial \theta^2} + \frac{\partial^2}{\partial \zeta^2},$$

and introducing the wave function Eq. (3.11) into Eq. (3.10) we obtain a non linear second-order differential equation also parametric in  $\alpha$

$$\phi'' + \frac{1}{\rho} \phi' - \frac{s^2}{\rho^2} \phi + \phi - \phi^3 - \alpha \left[ 2\phi'' \phi^2 + 2\phi'^2 + \frac{1}{\rho} \phi^2 \phi' \right] = 0. \quad (3.12)$$

We recognize in the equation the linear centrifugal term  $\propto s^2/\rho^2$  and the non-linear terms due to interaction between bosons. We have Dirichlet boundary conditions  $\phi(0) = 0$  since the wave function must vanish in the singularity and  $\phi(\infty) = 1$  for the normalization condition imposed. The equation is not analitically solvable but we can study the asintotic behavior of the solution, e.g. with polynomial trial functions. If for  $\rho \rightarrow 0$  we consider solutions of the type  $\rho^\tau$ , with  $\tau > 0$  a parameter to be found, we obtain that for all values of  $\alpha$  the solution goes as  $\phi \sim \rho^{|s|}$ ; notice that nevertheless we have no information on the value of  $\phi'$ . In a similar way, if for  $\rho \rightarrow \infty$  we try with solutions of the family  $1 - u\rho^{-\tau}$  with  $u$  another parameter we find the asymptotic behavior  $\phi \sim 1 - s^2/(2\rho^2)$ . Hence

$$\phi(r) \sim \begin{cases} \rho^{|s|} & \rho \rightarrow 0 \\ 1 - s^2/(2\rho^2) & \rho \rightarrow \infty \end{cases} \quad (3.13)$$

Furthemore it is important to underline the fact that the boundary condition at infinity impose a restraint to the parameter  $\alpha$ . In fact in Eq. (3.12) in the limit  $\rho \rightarrow \infty$  we can neglect the terms proportional to  $1/\rho$  and consider  $\phi' = 0$  (the solution is constant at infinity): we obtain the following differential equation to be considered in the range  $0 \leq \phi \leq 1$

$$\phi'' = -V'(\phi) = \frac{\phi(\phi^2 - 1)}{1 - 2\alpha\phi^2}, \quad (3.14)$$

for which we have the equilibria of interest  $\phi = 0$  and  $\phi = 1$  (our boundary conditions). The searched solution will be a curve between the points  $(0,0)$  and  $(1,0)$  in the phase space  $(\phi, \phi')$ . Unlike  $\phi = 0$ , which is always stable, studying  $\phi = 1$  we find that it is an equilibrium only if  $\alpha < 1/2$ . In fact the associated potential is

$$V(\phi) = \frac{2\alpha\phi^2 + (1 - 2\alpha) \ln(1 - 2\alpha\phi^2)}{8\alpha^2},$$

and, due to the presence of the logarithm, the potential diverges if  $\phi \rightarrow 1$  for values  $\alpha > 1/2$ .

Eq. (3.12) was solved numerically for a single-charged vortex with the software Mathematica (v 11.2) employing a *shooting method* to find with enough precision the appropriate (and unique) value of the initial condition  $\phi'(0)$  for which, varying the parameter  $\alpha$ , the solution satisfies the boundary condition at infinity. This is a so-called *separatrix* problem, because the solution divides the region of exponentially divergent solutions from oscillating solution which are affected by the attractor  $\phi \equiv 0$ , so very high precision is needed to obtain long range constant solutions. We notice that for  $\rho \sim 5$  the solutions are very close to the asymptotic behaviour of Eq. (3.13). As shown in Fig. (3.2), the shape of the vortex varies consistently with the new healing length accordingly to the relation

$$\xi' = \xi \sqrt{1 - \alpha}. \quad (3.15)$$

Hence, with regards to the GPE vortex profile ( $\alpha = 0$ ), the vortex widens for  $\alpha < 0$  and narrows for  $0 < \alpha < 1/2$ . The role of the healing length as the characteristic length for superfluid phenomena is definitely clear: a greater healing length means that the vortex will assume the constant profile at greater distances from the origin. Moreover we also got numerical evidence that no converging solutions exist for  $\alpha > 1/2$ . In conclusion we report a simple analytic expression which very well approximates the solutions, called the Padé approximation

$$f(\rho) = \frac{\rho}{\sqrt{\rho^2 + \lambda}}, \quad (3.16)$$

with the parameter  $\lambda$  which can be tuned accordingly to the value of  $\alpha$ : for the GPE a good choice is  $\lambda = 2$ .

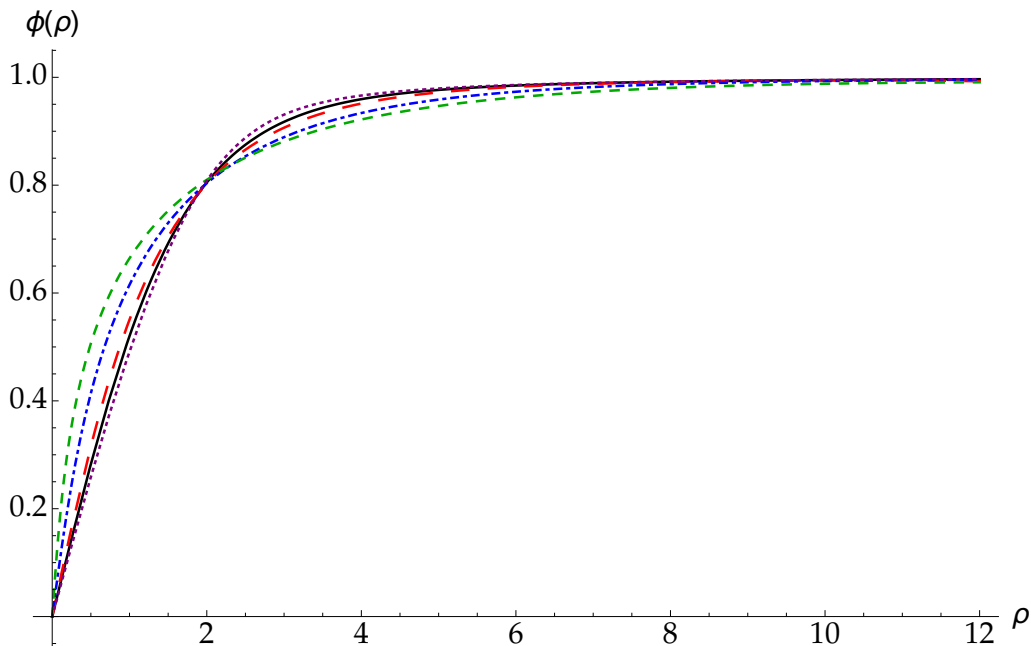


Figure 3.1: Profile of  $\phi(\rho)$  solution of Eq. (3.12) for different values of the parameter  $\alpha$  with appropriate values of  $\phi'(0)$ :  $\alpha = 0$  (GPE, solid black line,  $\phi'(0) \simeq 1.1664$ ),  $\alpha = -0.6$  (large-dashed red line,  $\phi'(0) \simeq 1.3389$ ),  $\alpha = +0.4$  (dotted purple line,  $\phi'(0) \simeq 1.0533$ ),  $\alpha = -3$  (blue dot-dashed line,  $\phi'(0) \simeq 2.1459$ ),  $\alpha = -7$  (short-dashed green line,  $\phi'(0) \simeq 4.1289$ ).

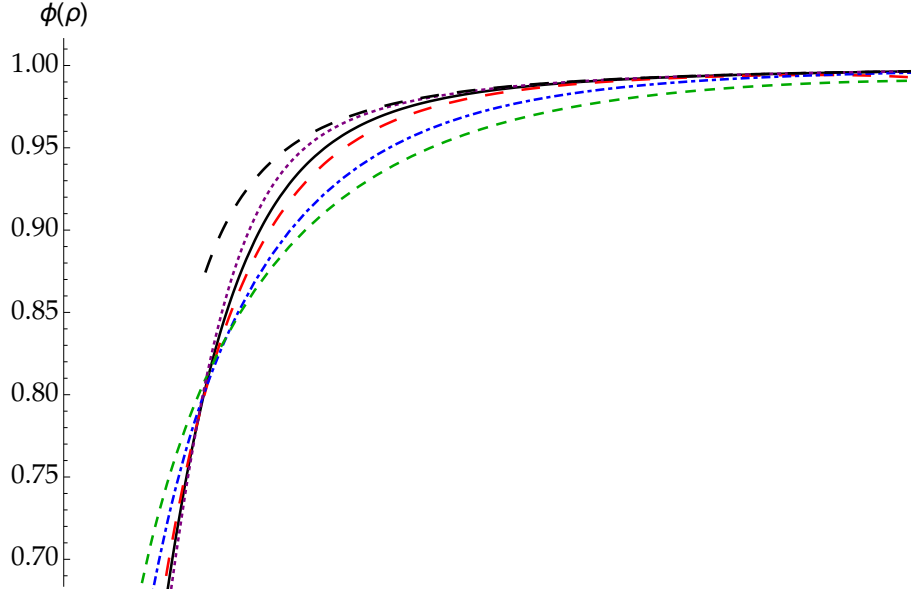


Figure 3.2: Detail of Fig. (3.1): notice that the vortex profile widens and crushes for  $\alpha < 0$  according to Eq. (3.15). Particularly we notice how this deformation is substantially "symmetric" with regards to the GPE profile. Furthermore all the solutions follow the asymptotic behavior for  $1 - 1/(2\rho^2)$  for  $\rho > 5$  (large-dashed black line).

### 3.3 Vortices in superfluid $^4\text{He}$

In He II the gas parameter  $na_s^3 \simeq 0.3$  is relatively large due to the strong interactions and high density of liquid helium. This leads to a very small healing length  $\xi \simeq 0.5 \div 1.0 \text{ \AA}$  and thus to difficulties in observing directly the structure of the vortex core. More accurate observations, together with Montecarlo calculations with realistic potentials [31] and the works of Berloff and Dalfovo [14], [12] show that, unlike vortices in weakly interacting Bose gases, the approach of the  $^4\text{He}$  fluid density to infinity is oscillatory rather than monotonic, the oscillations depending on the nature of the quasiparticle excitation spectrum. To prove this we consider the generalized non-local and non-linear Schrödinger equation we wrote in section 2.4 in order to describe the elementary excitations of superfluid helium. In the stationary form we have

$$\mu\psi = \left[ -\frac{\hbar^2}{2m}\nabla^2 + \int d^3\mathbf{r}' V(|\mathbf{r}' - \mathbf{r}|)|\psi(\mathbf{r}')|^2 + W|\psi|^{2(1+\nu)} \right] \psi. \quad (3.17)$$

To find the structure of a single-charged vortex one must solve Eq. (3.17) in cylindrical polar coordinates. Following [14], firstly we cast this equation into dimensionless variable with the same units chosen in section 2.4 absorbing the dimensionless constant  $n\xi^{-3}/\mu$  in  $V$

$$\nabla^2\psi + \left[ 1 - \int d^3\mathbf{r}' V(|\mathbf{r}' - \mathbf{r}|)|\psi(\mathbf{r}')|^2 - \chi|\psi|^{2(1+\nu)} \right] \psi = 0. \quad (3.18)$$

Now we introduce dimensionless cylindrical coordinates and we choose for the wave function the form of Eq. (3.11) with  $s = 1$ . Substituting in Eq. (3.18) we find

$$\begin{aligned} \phi''(\rho) + \frac{1}{\rho}\phi'(\rho) - \frac{1}{\rho^2}\phi(\rho) - \chi\phi(\rho)^{2\nu+3} - \int_0^\infty \rho' d\rho' \int_{-\infty}^\infty d\zeta' \\ \times \int_0^{2\pi} d\theta' \phi(\rho')^2 V\left(\sqrt{\rho^2 + \rho'^2 - 2\rho\rho' \cos(\theta - \theta') + (\zeta - \zeta')^2}\right) = 0. \end{aligned} \quad (3.19)$$

For the potential we choose the form of Eq. (2.26); integrating in  $\theta'$  and  $\zeta'$  we obtain the

non-local and non-linear differential equation

$$0 = \phi''(\rho) + \frac{1}{\rho}\phi'(\rho) - \frac{1}{\rho^2}\phi(\rho) - \chi\phi(\rho)^{2\nu+3} - \phi(\rho) \int_0^\infty \phi^2(\rho') \left\{ \frac{2\pi^{3/2}}{A} e^{-A^2(\rho^2+\rho'^2)} \right. \\ \left. \times [k_0(\rho, \rho')I_0(2A^2\rho\rho') - k_1(\rho, \rho')I_1(2A^2\rho\rho')] + \frac{2\pi^{3/2}}{B} \delta e^{-B^2(\rho^2+\rho'^2)} \right\} \rho' d\rho'. \quad (3.20)$$

The two functions  $k_0$  and  $k_1$  are given by

$$k_0(\rho, \rho') = \alpha + \frac{1}{2}\beta + \frac{3}{4}\gamma + \gamma A^4[(\rho^2 + \rho'^2)^2 + 4\rho^2\rho'^2] + A^2(\beta + \gamma)(\rho^2 + \rho'^2) \\ k_1(\rho, \rho') = 2A^2\rho\rho'(\beta + 2\gamma) + 4\gamma A^4\rho\rho'(\rho^2 + \rho'^2), \quad (3.21)$$

while  $I_0$  and  $I_1$  are the modified Bessel functions of order 0 and 1 that come from integration in  $\theta'$ . The solution has the same asymptotic behavior of Eq. (3.13) found for the MGPE case.

The equation was solved numerically with the software Mathematica upgrading the code employed in the previous section (see appendix): the integration in cylindrical coordinates and the presence of Bessel functions complicate the separatrix problem requiring much more precision in the shooting method. The solution can be found only iteratively since we have to choose a reasonable guess  $\phi_0$  to compute the integral and start the integration; then, after we have found a solution  $\phi_1$ , we recalculate the integral and so on, until convergence. As a starting guess we chose the simple Padé approximation Eq. (3.16) with  $\lambda = 1$ ; trials with other starting guesses led to the same converging solution but required more time. Usually 10-15 iterations and 2-5 hours of computational time on a standard laptop are enough to obtain a well-converged solution to  $\rho = 20$  depending on the parameters used. We solved Eq. (3.20) with the two sets of parameters found in section 2.4 with a fit to the dispersion curve: this is necessary because the vortex core density profile reflects the roton spectrum properties. Moreover the parameters were found with the constraint of Eq. (2.29) implying also the asymptotic limit of Eq. (3.20) to be satisfied. In Fig. (3.3) we show the solutions  $\phi^2$  found for  $\nu = 1$  and  $\nu = 2.8$ , together with the starting Padé approximation  $\phi_0$  and we compare them with the Montecarlo data from [31]: the feature of oscillating behavior of the density near the core is evident. As stated by Dalfovo [12] the data of Chester et al. can be fitted with the composition of a monotonic function and a damped Bessel function  $J_0(q_0r)$  where  $q_0 = 1.926 \text{ \AA}^{-1}$  is the wave vector of the roton minimum,  $0.9077\sqrt{1+\nu\chi}$  in adimensional units. We chose the form plotted in Fig. (3.3), here in dimensionless units  $\rho$ :

$$f(\rho) = \frac{\rho}{\sqrt{\rho^2 + 0.25}} \left[ 1 - 0.8e^{-0.4\rho} J_0(q_0\rho) \right]. \quad (3.22)$$

The link between the excitation spectrum and the vortex density profile is now clear. The boundary can be seen as a source of elementary excitations among which the roton excitations play the most important role: the liquid organize itself in quantized density "shells" separated by distance of order of the roton wavelength and amplitude which decreases as the distance from the boundary  $r = 0$  increases. That is why the requirement of a potential giving the right excitation spectrum is essential in reproducing quantized vortex in  $^4\text{He}$ .

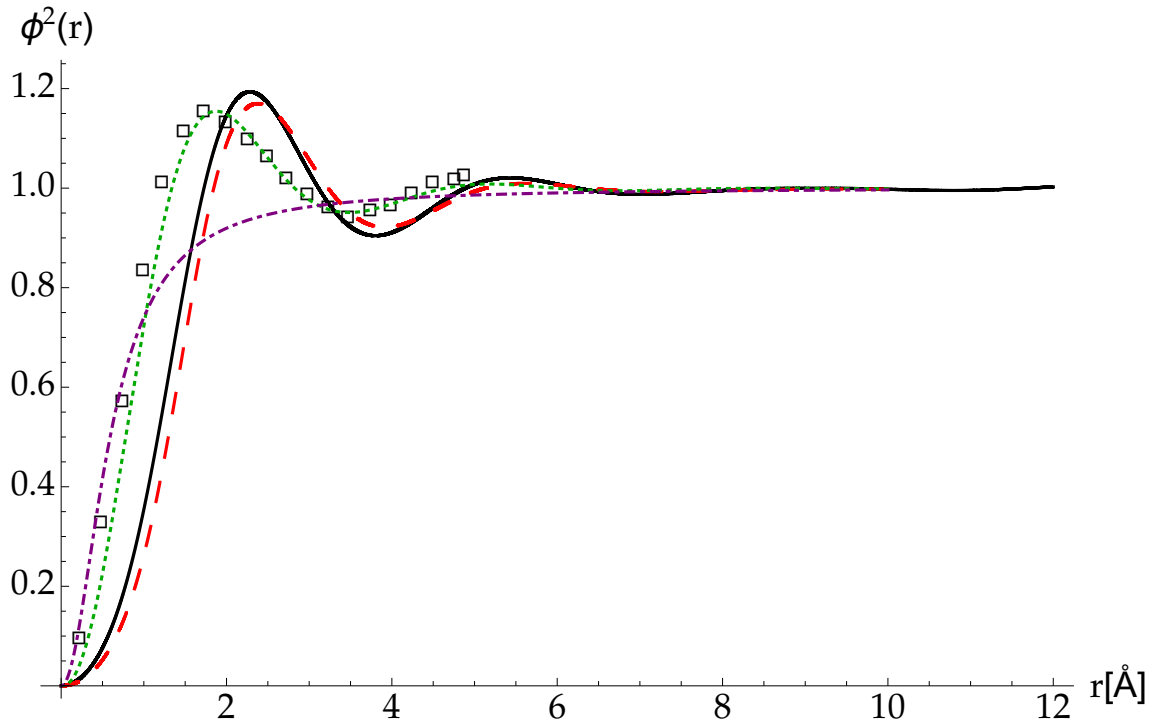


Figure 3.3: Quantized vortex in  ${}^4\text{He}$ . The numerical solutions of Eq. (3.20) with  $\nu = 1$  (solid black line) and  $\nu = 2.8$  (long-dashed red line) compared to Montecarlo data from [31], fitted with Eq. (3.22) (dotted green line) together with the Padé approximation, the initial guess  $\phi_0$  resembling the GPE vortex profile (dot-dashed purple line).

# Conclusions

In this work we reviewed the main properties of two of the most studied bosonic superfluid systems: ultra-cold alkali gases and  $^4\text{He}$ . Within a classical field formalism we wrote the Hartree equation, a single-particle differential equation, by which, with proper changes applied and hypothesis, we managed to describe the ground state properties, the quasiparticle excitation spectrum and quantized vortices, which are one of the most surprising and interesting phenomena in superfluidity. We also compared the results with experimental data with fair success.

The work on superfluid  $^4\text{He}$  may appear old-fashioned but the effort in modeling such system within a simple single-particle formalism, in parallel to other more complicated theories, can be useful to understand how the interparticle interactions can affect the nature of different quantum systems. For example, working with a non-local potential term as we did, inspired by the works of Berloff and Dalfovo, led us to develop tools and numerical techniques that can be useful to study condensates with strong dipolar interactions [33], very recently observed in BEC of  $^{52}\text{Cr}$ ,  $^{168}\text{Er}$  and  $^{164}\text{Dy}$ .

# Appendix - Mathematica codes

```
(* MGPE EQUATION *)
Clear[eps, end, \[Alpha]]
end = 12;
eps = 10^-5;
\[Alpha] = Rationalize[-5, 0]; (*set the parameter*)

eqnMGPE =
  u''[r] + u'[r]/r - u[r]/r^2 + u[r] -
  u[r]^3 - \[Alpha] D[r D[(u[r])^2, r], r] u[r]/r == 0;
sp = ParametricNDSolveValue[{eqnMGPE, u[eps] == 0, u'[eps] == up0,
  WhenEvent[u[r] > 11/10, {bool = 1, "StopIntegration"}],
  WhenEvent[{u[r] < 8/10, u[r] < 0}, {bool = 0,
  "StopIntegration"}]}, u, {r, eps, end + 3}, {up0, wp0},
  WorkingPrecision -> wp0, Method -> "StiffnessSwitching",
  Method -> {"ParametricSensitivity" -> None}, MaxSteps -> 100000];
bl = 9/10; bu = 10; imax = 200; wp = 75;
Row[{ProgressIndicator[Dynamic[ip], {0, imax}], "  "],
  ProgressIndicator[Dynamic[rm], {0, end}]}]
Do[bool = -1; bmiddle = (bl + bu)/2; s = sp[bmiddle, wp];
  rm = s["Domain"][[1, 2]];
  If[bool == 0, bl = bmiddle, bu = bmiddle];
  ip = i; If[bool == -1, Return[]], {i, imax}] // AbsoluteTiming
N[bmiddle, wp]
p0 = Plot[{s[r]}, {r, eps, Min[rm, end]}, PlotStyle -> {Black},
  AxesLabel -> {"\[Rho]", "\[Phi](\[Rho])"}, Axes -> True,
  AxesStyle ->
  Directive[Black, FontSize -> 18,
  FontFamily -> "TeX Gyre Pagella Math"],
  LabelStyle ->
  Directive[Black, FontSize -> 18,
  FontFamily -> "TeX Gyre Pagella Math"], ImageSize -> {Large},
  PlotRange -> All];

(* HARTREE EQUATION *)
Clear[A, B, a, b, d, \[HBar], M, n, \[Chi], \[Nu], v0, v1, v2, g0, g1,
  j, g00, g02, A\[Xi], \[Xi], X1, X0, X2, JJ, nOvera, V0];
Off[InterpolatingFunction::dmval]
eps = 10^-5;
end = 20;
V0 = 1;
\[HBar] = 1.054571800 10^-34; (*J*s*)
NA = 6.022 10^23 ;
M = 4.003 10^-3/NA; (*kg*)
e = 1.602176 10^-19;
kb = 1.3806503*10^-23;
c = 238;
as = 2.4 10^-10;
n0 = 0.0218 10^30;
v0 = 719 kb*10^-30;
v1 = 3.63 10^4 kb*10^-60;
v2 = 2.48 10^6 kb*10^-90;
qrot = 1.926 10^10;
```

```

Erot = 8.62 kb;
(*Equation parameters*)
\[Chi] = Rationalize[0.41893541674371876, 0]
\[Nu] = Rationalize[2.8, 0];
(*Potential parameters*)
A = Rationalize[1.8216676598426922, 0];
a = Rationalize[10.202043404551432, 0];
b = Rationalize[-16.006267177481995, 0];
d = Rationalize[1.7643890809636422, 0];
n = Rationalize[0.3832609060333534, 0];
B = Rationalize[0.6666019134179484, 0];

V[r_] = ((a + b A^2 r^2 + d A^4 r^4) Exp[-A^2 r^2] +
n Exp[-B^2 r^2]);
VT[q_] = 4 Pi *1/
64 Sqrt[\[Pi]] V0 ((16 a E^(-(q^2/(4 A^2))))/(A^2)^(3/
2) + (16 E^(-(q^2/(4 B^2))) n)/(B^2)^(3/
2) - (4 b E^(-(q^2/(4 A^2))) (-6 A^2 + q^2))/(A^2)^(5/
2) + (E^(-(q^2/(4 A^2))) d (60 A^4 - 20 A^2 q^2 +
q^4))/(A^6 Sqrt[A^2]));

Print["\[Xi]=", \[Xi] =
Sqrt[\[HBar]^2/ c^2 /2/M^2] Sqrt[1 + \[Nu] \[Chi]]>(*healing length*)
\[Mu] = \[HBar]^2/M/2/\[Xi]^2>(*chemical potential*)
Print["g00=",
g00 = N[SeriesCoefficient[Series[VT[q], {q, 0, 2}], 0]]]
Print["g02=",
g02 = N[SeriesCoefficient[Series[VT[q], {q, 0, 2}], 2]]]
Print["as=", as = N[M/(4 Pi \[HBar]^2) (g00 \[Mu]/n0)]>(*scattering length
*)
j[x_, r_] = 2 A^2 r x;
g0[x_, r_] =
a + b/2 + 3 d/4 + A^2 (b + d) (x^2 + r^2) +
d A^4 ((x^2 + r^2)^2 + 4 x^2 r^2);
g1[x_, r_] = j[x, r] (b + 2 d) + 4 d A^4 r x (r^2 + x^2);
jb[x_, r_] = 2 B^2 r x;
g0b[x_, r_] = n
endp = end + 1;
s[0][x_] = x/Sqrt[x^2 + 1];
F[0] = Interpolation@
Rationalize[
Table[{r,
2 (Pi)^(3/2)/
A E^(-A^2 (r^2)) NIntegrate[(x s[0][
x]^2 E^(-A^2 x^2) (g0[x, r] BesselI[0, j[x, r]] -
g1[x, r] BesselI[1, j[x, r]])), {x, 0, 30},
WorkingPrecision -> 30, PrecisionGoal -> 8] +
2 (Pi)^(3/2)/
B E^(-B^2 (r^2)) NIntegrate[(x s[0][
x]^2 E^(-B^2 x^2) (g0b[x, r] BesselI[0, jb[x, r]])), {x,
0, 30}, WorkingPrecision -> 30, PrecisionGoal -> 8]}, {r, 0,
endp, 1/10}], 0];
Print["Asymptotic test =", N[1 - \[Chi] - F[0][end]]] (*check if it is
close enough to 0*)
Print["\[Chi]=", N[\[Chi]]]

mmin = 1; mmax = 10; imax = 200; wp = 60; (*iteration parameters: change if
needed*)
Row[{Dynamic[m], " ", ProgressIndicator[Dynamic[ip], {0, imax}],
" ", ProgressIndicator[Dynamic[rm], {0, end}]}]
AbsoluteTiming[
Do[eqn = u''[r] + u'[r]/r - u[r]/r^2 +
u[r] - \[Chi]*u[r]^(2 \[Nu] + 3) -
u[r] (F[m - 1][r] + F[Max[m - 2, 0]][r])/2 == 0;
sp = ParametricNDSolveValue[{eqn, u[eps] == eps up0,
u'[eps] == up0,

```



```

WhenEvent[
  u[r] > s[0][end] + 1/5 (1 - r/endpoint) + 1/200 (r/endpoint), {bool =
    1, "StopIntegration"}],
WhenEvent[{u[r] < s[0][end] - 1/5 (1 - r/endpoint) - 1/200 (r/endpoint),
  u[r] < 1/5}, {bool = 0, "StopIntegration"}]],
u, {r, eps, endpoint}, {up0, wp0}, WorkingPrecision -> wp0,
Method -> "StiffnessSwitching",
Method -> {"ParametricSensitivity" -> None},
MaxSteps -> 100000];
bl = 1/5; bu = 2;
Do[bool = -1; bmiddle = (bl + bu)/2; st = sp[bmiddle, wp];
  rm = st["Domain"][[1, 2]];
  If[bool == 0, bl = bmiddle, bu = bmiddle]; ip = i;
  If[bool == -1, Return[]], {i, imax}];
s[m] = st; N[bmiddle, wp];
F[m] =
Interpolation@
Rationalize[
Table[{r,
  2 (Pi)^(3/2)/
  A E^(-A^2 (r^2)) NIntegrate[(x Piecewise[{{s[m][x],
    eps < x < end}}],
    s[0][x]]^2 E^(-A^2 (x^2)) (g0[x, r] BesselI[0,
      j[x, r]] - g1[x, r] BesselI[1, j[x, r]])), {x, 0,
    30}, WorkingPrecision -> 30, PrecisionGoal -> 8] +
  2 (Pi)^(3/2)/
  B E^(-B^2 (r^2)) NIntegrate[(x Piecewise[{{s[m][x],
    eps < x < end}}],
    s[0][x]]^2 E^(-B^2 x^2) (g0b[x, r] BesselI[0,
      jb[x, r]])), {x, 0, 30}, WorkingPrecision -> 30,
    PrecisionGoal -> 8]}, {r, 0, endpoint, 1/10}], 0];
Print["bmiddle ", m, ": ", N[bmiddle]], {m, mmin, mmax}];
Plot[Evaluate@Table[s[m][r], {m, mmax - 5, mmax}], {r, eps, endpoint},
  PlotRange -> All, AxesLabel -> {r, u}, ImageSize -> Large,
  LabelStyle -> {Black, Bold, Medium}]
Plot[Evaluate@Table[F[m][r], {m, mmax - 5, mmax}], {r, 0, endpoint},
  PlotRange -> All, AxesLabel -> {r, "F"}, ImageSize -> Large,
  LabelStyle -> {Black, Bold, Medium}]
Plot[Evaluate@Table[s[m][r]^2, {m, mmax - 5, mmax}], {r, 0.01, endpoint},
  PlotRange -> All, AxesLabel -> {"r", "n(r)"}, ImageSize -> Large,
  AxesStyle ->
  Directive[Black, FontSize -> 17,
    FontFamily -> "TeX Gyre Pagella Math"],
  LabelStyle ->
  Directive[Black, FontSize -> 17,
    FontFamily -> "TeX Gyre Pagella Math", ImageSize -> {Large},
  PlotRange -> All]
Print["\[Xi]=", \[Xi] =
  Sqrt[\[HBar]^2/ c^2 /2/M^2] Sqrt[1 + \[Nu] \[Chi]]]
psol = Plot[s[mmax][r/(10^10 \[Xi])]^2, {r, 10^-4, 10},
  PlotRange -> All]

```

# Bibliography

- [1] P. Kapitza, Viscosity of liquid helium below the  $\lambda$  point, *Nature* **141**, 74 (1938).
- [2] F. London, On the Bose-Einstein condensation, *Phys. Rev* **54**, 947 (1938).
- [3] L. Landau, The theory of superfluidity of helium II, *J. Phys. USSR* **5**, 71 (1941).
- [4] L. Tisza, Transport phenomena in helium II, *Nature* **141**, 913 (1938).
- [5] L. Onsager, *Nuovo Cimento Suppl.* **6**, 249 (1949).
- [6] R.P. Feynman, Application of quantum mechanics to liquid helium, *Progress in Low Temperature Physics* **1**, 17 (Gorter, C.J. ed., Amsterdam, North-Holland, 1955).
- [7] M. H. Anderson, J.R. Ensher, M. R. Matthews, C. E. Wieman and E. A. Cornell, *Science* **269**, 198 (1995).
- [8] K. B Davis, M. O. Mewes, M. R. Andrews, N. J. van Druten, D. S. Durfee, D. M. Kurn and W. Ketterle, *Phys. Rev. Lett.* **75**, 3969 (1995).
- [9] A. Marte, T. Volz, J. Schuster, S. Dürr, G. Rempe, E. G. M. van Kempen, and B. J. Verhaar, *Phys. Rev. Lett.* **89**, 283202 (2002).
- [10] E. P. Gross, Structure of a quantized vortex in boson systems, *Nuovo Cimento* **20**, 454 (1961).
- [11] L. P. Pitaevskii, Vortex Lines in an Imperfect Bose Gase, *Zh. Eksp. Teor. Fiz.* **40**, 646 *Sov. Phys. JETP* **13**, 451 (1961).
- [12] F. Dalfovo, *Phys. Rev. B* **46**, 9 (1992).
- [13] F. Dalfovo, A. Latri, L. Pricauptenko, S. Stringari, J. Treiner, *Phys. Rev. B* **52**, 1193 (1995).
- [14] N. G. Berloff, P. H. Roberts, *J. Phys. A: Math. Gen.* **32**, 5611 (1999).
- [15] R. A. Aziz, V. P. S. Nain, J. S. Carley, W. L. Taylor, and G. T. McConville, An accurate intermolecular potential for helium, *The Journal of Chemical Physics* **70**, 4330 (1979).
- [16] J. F. Annett, *Superconductivity, Superfluids and Condensates* (Oxford University Press, Bristol, 2004).
- [17] A. J. Leggett, *Rev. Mod. Phys.* **73**, 307 (2001).
- [18] D. Vautherin and D. M. Brick, *Phys. Rev. C* **5**, 626 (1972).
- [19] N. G. Berloff, M. Brachet, and N. P. Proukakis, Modeling quantum fluid dynamics at nonzero temperatures *PNAS* **111**, 1, 4675 (2014).
- [20] H. Fu, Y. Wang, and B. Gao, *Phys. Rev. A* **67**, 053612 (2003).
- [21] A. Cappellaro, L. Salasnich, *Phys. Rev. A* **95**, 033627 (2017).

- [22] H. T. C. Stoof, D. B. M. Dickersheid, K. Gubbels, *Ultracold Quantum Fields* 223 (Springer, Berlin, 2009).
- [23] L. Landau, E. M. Lifshitz, L. P. Pitaevskii, *Course of Theoretical Physics Vol. 9, Theory of the Condensed State, Part 2*, (Pergamon press, Oxford, 1980).
- [24] C. F. Barenghi, N. G. Parker, *A Primer on Quantum Fluids* (Springer, 2016).
- [25] L. Salasnich, *Quantum Physics of Light and Matter* (Springer, Berlin, 2014).
- [26] J. Steinhauer, R. Ozeri, N. Katz, and N. Davidson, *Phys. Rev. Lett.* **88**, 120407 (2002).
- [27] R. J. Donnelly, J. A. Donnelly, R. N. Hillst, *J. Low Temp. Phys.* **44**, 471 (1981).
- [28] N. G. Berloff, P. H. Roberts, *Phys. Lett. A* **274**, 69-74 (2000).
- [29] N. G. Berloff, *J. Low. Temp. Phys.* **116**, 5 (1999).
- [30] A. L. Fetter, *Quantum Theory of Many-Particle Systems*, 481 (McGraw Hill, New York).
- [31] G. V. Chester, R. Metz, and L. Reatto, *Phys. Rev.* **175**, 275 (1968).
- [32] L. Pitaevskii, S. Stringari, *Bose-Einstein Condensation*, (Clarendon press, Oxford, 2003).
- [33] R. Kishor Kumar, Luis E. Young-S., Dušan Vudragović, Antun Balaž, Paulsamy Muruganandam, S. K. Adhikari, arXiv:1506.032[cond-mat.quant-gas] (2015)